Depression of Lead-activated Sphalerite by Sodium Hydrogen Phosphate for Red Dog Mine Operation

by

Aijing Wang

A thesis submitted in partial fulfillment of the requirements for the degree of

Master of Science

in

Chemical Engineering

Department of Chemical and Materials Engineering

University of Alberta

Abstract

The inadvertent activation of sphalerite by lead ions have been noticed and studied for decades. In this study, flotation behavior of sphalerite upon lead activation was studied. Sodium hydrogen phosphate was applied as a main depressant to test its effect on improving Pb-Zn selectivity. Surface characterizations, such as Fourier transform infrared (FTIR) spectroscopy, X-ray photoelectron spectroscopy (XPS), and Time-of-flight secondary ion mass spectroscopy (ToF-SIMS) were conducted to understand the basic mechanism happening on the sphalerite surface.

Sphalerite showed a strongly enhanced floatability with xanthate after Pb activation. The addition of sodium hydrogen phosphate depressed the Pb-activated sphalerite flotation and did not put impacts on galena flotation. However, its performance was unsatisfactory during the mixed mineral flotation. XPS and ToF-SIMS analyses suggested that sodium hydrogen phosphate had limited ability to complex Pb ions, rather it worked mainly by oxidizing PbS to PbO. To compensate the limited depressing ability of sodium hydrogen phosphate in a mixed mineral system, zinc sulfate was introduced prior to sodium hydrogen phosphate addition. The combination usage of the two reagents showed good selectivity when both of their concentration was at 10^{-5} M, resulting in a Zn% recovery of 55.0% and a Pb% recovery of 90.2%.

Acknowledgements

I would like to express my sincere gratitude and appreciation to:

- My supervisors, Dr. Qingxia (Chad) Liu and Dr. Qi Liu for their support and guidance throughout my research study.
- Dr. Anqiang He, Dr. Shihong Xu, Dr. Nancy Zhang from nanoFAB center for the provision of laboratory equipment and services.
- Dr. Mingli Cao, Carl Corbett and Jie Ru for the material and equipment setup, training of laboratory equipment and allowing me to use the mineral processing lab.
- Dr. Jing Liu, Bailin Xiang, Hanrui Zheng, Hao Huang, Cassie Zhao for their help and suggestions in my experiments. I would like to show my appreciation especially to Chao Qi, who has guided me and provided me with a lot of ideas on my research study. I would also like to express my appreciation to all the other colleagues in our group.
- Teck Resource Ltd. and Natural Science and Engineering Research Council of Canada (NSERC) for the financial support.

Finally, I would like to thank my parents who have provided enduring support to me over these years. Without you I cannot go this far. I also want to thank all my other families and my friends for their supports and encouragement to me.

Table of Contents

List of Tables

List of Figures

Chapter 1 Introduction

1.1 Principles of flotation

Sphalerite, mainly composed of zinc sulfide, is a naturally abundant mineral which is a major source of zinc metal. The sphalerite is commonly found its co-existence with other sulfide minerals, such as galena (PbS), pyrite (FeS_2), chalcopyrite ($CuFeS_2$), and so on. Flotation technique is widely applied in industry to separate sphalerite from other valuable and gangue minerals. In general, separation by flotation is achieved based on different hydrophobicity of the mineral surface. In practice, the minerals are crushed and grinded into fine particles and mixed with feed water, then the slurry is sent through a flotation column with air bubbling from the bottom. The hydrophobic mineral particles can attach to the air bubbles and be carried up, whereas the hydrophilic particles will remain in the slurry. In such a manner the hydrophobic minerals could be separated from the rest of unwanted minerals.

1.1.1 Collector adsorption

Many of the sulfide minerals are not naturally floatable since their mineral surfaces are not intrinsically hydrophobic. Collector is introduced during the floatation process to increase the surface hydrophobicity. Xanthates, as the most widely used collectors in sulfide flotation since 1923 (Leja, 1982), are derivatives of carbonic acid, H_2CO_3, by replacing two oxygens by sulfur and one hydrogen by alkyl groups. The chemical structure of xanthate is shown in Figure 1.1.

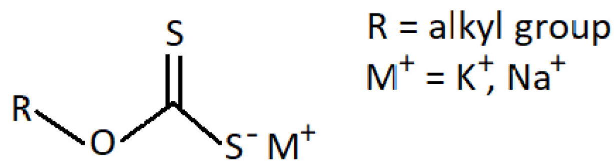

Figure 1.1 Chemical structure of xanthate salt

Some of the commonly used xanthates are:

- sodium ethyl xanthate (SEX), $CH_3CH_2OCS_2Na$,
- potassium ethyl xanthate (KEX), $CH_3CH_2OCS_2K$,
- sodium isopropyl xanthate (SIPX), $(CH_3)_2CHOCS_2Na$
- sodium isobutyl xanthate (SIBX), $(CH_3)_2CHCH_2OCS_2Na$
- potassium amyl xanthate (PAX), $CH_3(CH_2)_4OCS_2K$

When adsorbing onto the sulfide mineral surface, the $-CS_2$ group can react with the surface sites and expose the alkyl group (non-polar tail) to the liquid phase, rendering the mineral surface hydrophobic. In general, xanthates with longer alkyl chains will have lower solubility products with metal ions, as can be shown in Table 1.1, and therefore result in better flotation behavior. Although longer chain xanthates are more powerful, they may sacrifice some selectivity (Leja, 1982).

Table 1.1 Logarithm of solubility products (pK_{sp}) of metal xanthate complexes and metal hydroxides (Rao & Leja, 2004)

Ligand	Zinc (II)	Lead (II)	Copper (I)	Silver (I)
Ethyl xanthate	-8.31	-16.77	-19.28	-18.30
Butyl xanthate	-10.43		-20.33	
Hexyl xanthate	-12.90			-20.40
Octyl xanthate	-15.82		-23.06	-21.86
Hydroxide	-16.79	-16.09	-14.70	-7.39

1.1.2 Sphalerite activation

Activation, defined by Finkelstein and Allison (1976), is a process where the mineral surface is modified so that it can react more easily and strongly with a collector. From Table 1.1 it can be observed that zinc has relatively large solubility products (K_{sp} values) with xanthates when comparing with zinc hydroxide or other metal xanthates. This suggests that zinc xanthate products are highly soluble, so that even after treating with xanthate, sphalerite is still not floatable. Therefore, sphalerite needs to be activated by metal ions such as lead, copper or silver, which can form less soluble xanthate products to render the surface hydrophobic.

Table 1.2 Solubility product constants of metal sulfides (Dean, 1999)

Compound Formula	K_{sp}	pK_{sp}
ZnS	2.5×10^{-22}	21.60
PbS	8.0×10^{-28}	27.10
Cu_2S	2.5×10^{-48}	47.60
Ag_2S	6.3×10^{-50}	49.20

*The data refer to various temperatures between 18°C to 25°C.

Table 1.2 shows the solubility products of some common metal sulfides. Taking lead activation under acidic condition as an example, exchange reactions between lead and zinc cations occur upon the sphalerite surface.

$$Pb^{2+} + ZnS \rightleftharpoons PbS + Zn^{2+}$$

The equilibrium constant for this exchange reaction can be calculated as the following:

$$K = \frac{[Zn^{2+}]}{[Pb^{2+}]} = \frac{K_{sp(ZnS)}}{K_{sp(PbS)}} = \frac{2.5 \times 10^{-22}}{8.0 \times 10^{-28}} = 3.125 \times 10^{5}$$

The large equilibrium constant indicates that the ion exchange reaction is likely to occur in ambient environment. The surface will then behave more like PbS surface and allows xanthate adsorption more easily, hence facilitating the mineral flotation.

$$PbS + 2EX^{-} \rightleftharpoons Pb(EX)_2 + S^0 + 2e^{-}$$

1.2 Description of Red Dog mine operation

Red Dog mine is located 1,000 km northwest of Anchorage, Alaska. Operated by Teck Alaska, Inc., a subsidiary of Teck Resources Limited. Red Dog mine is one of the world's largest zinc mines, both in terms of reserves and its zinc production. Starting operation since 1989, the Red Dog mine nowadays can process ore milled over 4,000 kilotons with 15.0% grade of Zn and 4.2% grade of Pb per annum. The total zinc metal produced during 2016 was about 583 kilotons and 705 kilotons for lead metal. (Letient, 2017)

Figure 2.1 shows a simplified illustration of the Red Dog plant operation. The crushed ores are first sent to the grinding mill together with fresh water and plant recycling water to make mineral slurries. The ores are grinded into fine particles with majority of the particle size under 65 µm. The slurries then go through the lead flotation rougher, wherein galena (PbS) can be floated by air bubbles with facilitation of xanthate addition and sphalerite (ZnS) is depressed with addition of zinc sulfate ($ZnSO_4$). The floated mineral, called as lead concentrate, is separated from the rest of the ores in such a way and will be later sent to smelter for lead metal extraction. Ores that are not floated in the lead rougher, called as tails or tailings, are sent for regrinding into smaller particle size (less than 20 µm). These particles go through the zinc flotation process. During the zinc flotation, copper sulfate ($CuSO_4$) is added to activate the sphalerite surface; xanthate is also furtherly added so that sphalerite can be floated as zinc concentrate. The tailings undergo tailings treatment, whereby lime and flocculants are introduced to aggregate the very fine particles into clumps, called as flocs, to assist the precipitation of these remaining gangues in the tailing pond. During the whole lead-zinc separation process, the pH of the pulp solution remained weakly acidic between 5.6 - 6.7, and for the flotation processes the pH is maintained roughly between 6.2 - 6.5.

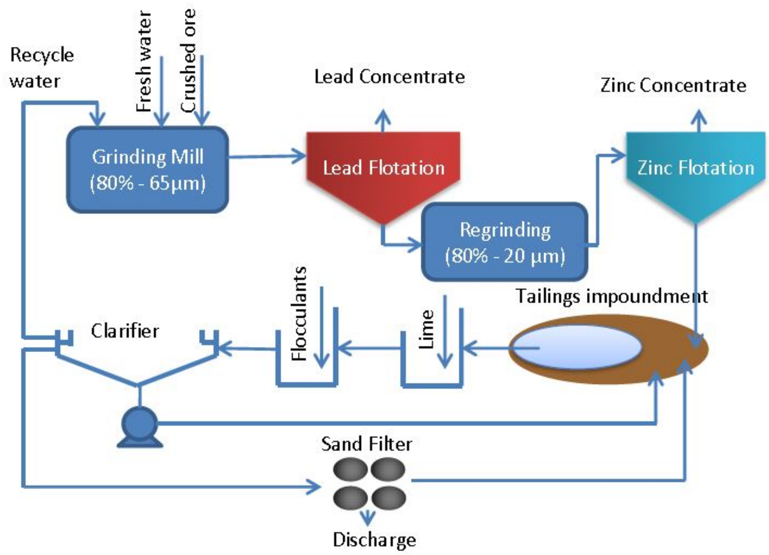

Figure 1.2 Schematic of Red Dog plant (Deng, 2013)

1.3 Objectives of the study

Flotation of sphalerite has been studied by decades. However, the activation mechanism of sphalerite, especially by lead ions, is still under some disputes. Also, although many depressants have been found effective in depressing sphalerite during lead flotation in different studies, they are rarely applied in real plant flotation. Based on these existing problems, this study will conduct research focusing on the following aspects:

1) The activation mechanism of sphalerite by lead ions in mildly acidic condition

A common problem happening during the lead-zinc flotation separation is the inadvertent activation of sphalerite by lead ions. Galena and anglesite can release lead ions (Pb^{2+}) and lead hydroxide ($Pb(OH)^{+}$) into the weakly acidic pulp solution. These aqueous lead ions will activate the sphalerite surface in nature and enhance sphalerite flotation in the lead rougher, wherein sphalerite should be depressed. The inadvertent activation of sphalerite will cause a misreport of zinc into the lead concentrates, and a decrease in the zinc recovery in the later zinc flotation. To understand the flotation behavior and the activation mechanism of sphalerite by the lead ions, micro-flotations are conducted in mildly acidic condition (pH 6.5), lead nitrate and potassium ethyl xanthate will be used as activator and collector respectively. Surface characterizations, such as Fourier transform infrared spectroscopy (FTIR), X-ray photoelectron spectroscopy (XPS), and Time-of-Flight Secondary Ion Mass Spectroscopy (ToF-SIMS) are conducted in order to investigate the surface interactions.

2) Depression of lead-activated sphalerite by sodium hydrogen phosphate

Although researchers have spent decades to seek effective depressant to be applied in lead-zinc flotation separation, seldom of them is accepted by the industry. One common depressant in use nowadays is zinc sulfate; however, it cannot completely depress sphalerite. Therefore, a new depressant with stronger depressing power is urgently needed. Our study has found sodium hydrogen phosphate effective in depressing the sphalerite flotation in weakly acidic condition, especially when it's in combination with zinc sulfate. Micro-flotation tests are conducted to see the depressing effects, and surface analyses are carried out to help understand the deactivation mechanism by sodium hydrogen phosphate. Sphalerite-galena mixed flotation is also carried out to study the selectivity of the depressant.

1.4 Organization of this thesis

This thesis consists of six chapters.

Chapter 1: This chapter gives an overall introduction of the research background. The principle of flotation and flotation operation are briefly introduced. The research objectives are outlined.

Chapter 2: This chapter provides literature review on previous studies regarding sphalerite flotation by other researchers.

Chapter 3: In this chapter, materials and techniques applied in this research study are introduced. The fundamentals and experiment procedures are described in detail.

Chapter 4: This chapter demonstrates the micro-flotation results. Sphalerite flotation and sphalerite-galena mixed flotation under weakly acidic condition are both conducted. The effect of lead activation, depression by sodium hydrogen phosphate are examined respectively. Mixed flotation is conducted to study the selectivity of sodium hydrogen phosphate.

Chapter 5: In this chapter, several surface characterization techniques are applied to explain the activation and deactivation mechanisms occurring on the sphalerite surface.

Chapter 6: This chapter summarizes the conclusions, the significance of this study, and suggestions for the future work.

1.5 References

Dean, J. A. (1999). *Lange's Handbook of chemistry* (5th ed.). McGraw-Hill, Inc.

Deng, M. (2013). *Impact of gypsum supersaturated solution on the flotation of sphalerite*. University of Alberta.

Finkelstein, N. P., & Allison, S. A. (1976). *Flotation, A.M. Gaudin Memorial Volume*. (M. C. Fuerstenau, Ed.). New York, N.Y.

Leja, J. (1982). *Surface Chemistry of Froth Rotation* (1st ed.). New York: Plenum Press.

Letient, H. (2017). Red Dog Operations. Retrieved from http://www.reddogalaska.com/

Rao, S. R., & Leja, J. (2004). *Surface Chemistry Surface Chemistry of Froth Flotation* (2nd ed.). New York: Springer Science+Business Media.

Chapter 2 Literature Review

2.1 Lead activation of sphalerite and xanthate adsorption

Basilio et al. (1996) performed a series of spectroscopic analyses to prove the inadvertent activation of sphalerite by lead ions during galena flotation. The flotation results showed a significant amount of sphalerite floated in the second lead rougher. The much higher surface Pb/Zn atomic ratio comparing with the bulk Pb/Zn ratio suggested that sphalerite surface was activated by lead ions. The Pb/Zn ratio was also compared when treated with different conditioning solutions. The sphalerite specimen had considerably higher Pb/Zn ratio when it was treated with lead sulfate solution or lead-containing process water, comparing with the one treated with distilled water. It was suggested that the aqueous lead ions were mainly responsible for the activation. When sphalerite was treated with lead sulfate and potassium amyl xanthate, the Fourier Transform Infrared (FTIR) spectrum showed the presence of lead xanthate (PbX_2) and dixanthogen (X_2), but no presence of zinc xanthate was observed, which also indicated the lead activation of the sphalerite surface.

Mielczarski (1986) studied the self-activation of sphalerite by its self-bearing lead impurity. He compared two sphalerite samples, one with higher lead content (1.15 wt%) and the other with lower lead content (0.32 wt%). The specimen with lower lead content performed similarly to synthetic ZnS in both flotation results and surface characterizations, showing low floatability and very small amount of xanthate adsorption on the surface. While the sphalerite sample with higher lead content demonstrated different results and its performance was found dependent on pH of the solution. The rate of xanthate adsorption was found greatest under weakly acidic condition. The adsorption rate decreased as the medium became basic and there was rarely xanthate adsorption above pH 9, which was different from Laskowski et al. (1997)'s study, stating a significant increase in the flotation rate constant in alkaline conditions. At near neutral pH (pH 6.5 - 7.1), lead ethyl xanthate was formed; however, it did not provide floatability to sphalerite. This could contribute to the precipitation of spots and clusters of lead ethyl xanthate on the surface. Ethyl dixanthogen and elementary sulfur, which are two possible products formed on sphalerite surface and contribute to floatability as proposed by many researchers, were not determined in this study.

Trahar et al. (1997) studied the lead activation of sphalerite in both mildly acidic and moderately alkaline conditions. They also studied the effect of presence of ethyldiaminetetraacetic acid (EDTA) on flotation behavior. They observed that sphalerite did not float by adding lead ions alone without the presence of xanthate as collector. With addition of xanthate, sphalerite recovery increased with ascending amount of xanthate addition. At pH 9 with a fixed amount of potassium ethyl xanthate (KEX) of 4.55×10^{-5} M, the flotation recovery increased as lead ions increased, reaching its optimum at 200 - 400 ppm, and dropped down with further addition. The decreased recovery was due to the participated xanthate at higher pH values. At higher pH the decline of recovery was also caused by xanthate-hydroxyl competition occurred. The addition of EDTA did not alter the sphalerite floatability at pH 4, but greatly decreased its recovery at pH 7 - 9. The PbS layer was found dissolved at pH 9. Trahar et al. concluded that at mildly acidic condition the activator was lead ion and the activation mechanism was by exchange reaction; whereas in alkaline condition the activator was lead hydroxide; however, the activation mechanism remained unclear.

2.2 Activation mechanism under acidic condition

There are three activation mechanisms that are proposed under acidic condition:

- Pb/Zn exchange
- Formation of Zn-O-Pb surface product via reaction of lead oxide/hydroxide and ZnS
- Filling the empty cation sites by Pb ions

Among the above proposed mechanisms, the first exchange mechanism was mostly accepted. Each of these mechanisms will be reviewed by the following content.

2.2.1 Pb/Zn exchange

The Pb/Zn exchange mechanism is the mostly accepted mechanism under acidic condition. Finkelstein and Allison (1976) and Ralston and Healy (1980) studied the activation mechanism of highly pure synthetic zinc sulfide by lead ion in weakly acid media (pH 4 - 6.5). They found the first activation stage was completed within 1 minute and was logarithmically dependent on time. The initial rapid activation stage was summarized as the following: Aqueous Pb^{II} ions first diffuse to the ZnS surface, then make adsorption to the surface. The adsorbed Pb^{II} ions transfer from the adsorbed sites to the lattice sites, which is slow and rate determining for the initial activation stage. The Zn^{2+} ions that are substituted by Pb^{II} ions then transfer from lattice sites to the surface, desorb from the ZnS surface and diffuse into the solution. The first stage is followed by the second slow stage which was completed for more than 2 hours. The rate equation for the second stage could not be defined. The lead uptake was found to be dependent on pH, initial Pb^{II} concentration and zinc sulfide concentration. In their following study (Ralston, Alabaster, & Healy, 1981) they detected elemental sulfur using electron spectroscopy for chemical analysis (ESCA), and concluded that redox reactions could occur after the initial exchange reaction, as S^0 was detected on the ZnS surface with lead activation. The acceptor state introduced by Pb^{II} is below the Fermi level and close to the valance band, so that the electrons are easily promoted from valance band to acceptor state by thermal energy kT, according to the following reactions:

$$Pb^{2+}_{surface} + e^{-} \rightleftharpoons Pb^{+}_{surface}$$

$$1/_2\, S^{2-}_{surface} \rightleftharpoons 1/_2\, S^{0}_{surface} + e^{-}$$

The S^0 formed was found unstable and its stability decreases with increasing pH. The S^0 slowly decomposes into sulfur-hydrogen-oxygen compounds ($S_xH_yO_z$) under mildly acidic media and decomposes rapidly at alkaline conditions.

Popov et al. (1989) performed Internal Reflection (IR) spectroscopy to study the adsorption kinetics of ethyl xanthate in the presence of lead ions. The IR absorption bands of lead ethyl xanthate were hard to observe when the sphalerite was treated with sodium ethyl xanthate alone but observed when the sphalerite was treated with lead ions first. The intensity of the band increased with increasing lead ion concentration up to 7.0×10^{-5} mol/L. In weakly acid medium (pH 5 - 6) the near-equilibrium stage was reached when the sphalerite was treated with lead ions for 15 minutes, whereas in alkaline medium (pH 8 - 9) the activation time was about 40 min. This observation was well correlated with Ralston and Healy’s conclusions, which indicated that the activation mechanism was fast by exchange reaction of lead and zinc ions in acid conditions, and slow in alkaline media by reaction of $Pb(OH)_2$ on the sphalerite surface. (Ralston et al., 1981; Ralston & Healy, 1980a, 1980b) For both acidic and alkaline conditions, the collection time was found efficient at

15 minutes.

Laskowski et al. (1997) combined electrokinetic and flotation tests to investigate the activation mechanism of sphalerite activation by copper and lead ions. They found out that under acidic condition, the sphalerite surface was easily activated by either Cu^{2+} or Pb^{2+} ions within a short amount of time, of which the mechanism can be described by the following equation:

$$M^{2+}_{(aq)} + ZnS_{(s)} \rightleftharpoons MS_{(s)} + Zn^{2+}_{(aq)}$$

Where $M^{2+}_{(aq)}$ represents divalent metal ions such as Cu^{2+} or Pb^{2+}, and $MS_{(s)}$ is the surface activation product which is “flotation-active”.

Houot and Raveneau (1992) found the Pb/Zn exchange ratio to be 1.22 during the aeration of galena and sphalerite instead of the theoretical 1.0. They also observed that during the aeration of the mineral mixture, the quantity of lead fixed on the sphalerite surface depended on the pH level of the solution, which varied slightly along pH 6 - 10, and reached maximum at pH 12. The electron spectroscopy for chemical analysis (ESCA) showed that the amount may accounted up to 30% of the cationic sites of the first ten atomic layers. They suggested that for clean mineral surfaces cleaned by either EDTA (ethylene diaminetetraacetic acid) washing or acid leaching, Pb/Zn exchange reaction represented the dominant activation mechanism; whereas for oxidized surface, there existed competition between Pb/Zn exchange and lead oxide coating. Rapid activation kinetics were observed.

Rashchi et al. (2002) summarized the lead activation mechanism of sphalerite over pH ranges as shown in Fig 2.1. Below pH 7, the significant activation was achieved by Pb/Zn ion exchange, and xanthate adsorbed directly on the lead ion that has replaced onto the sphalerite surface. The activation was progressively less as pH value increased, and sphalerite performed no floatability beyond pH 11. From pH 7 - 10, the activation mechanism was described as the following equation (Bernasconi, cited Houot and Ravenau, 1992):

$$SZnOH + PbOH^{+} \longrightarrow SZn - O - Pb^{+} + H_2O$$

Under alkaline condition, lead hydroxide ($Pb(OH)_2$) was deposited on the sphalerite surface, which is hydrophilic and depressed sphalerite flotation. Zinc hydroxide ($Zn(OH)_2$) maybe also formed and contributed to the diminishing flotation. Rashchi et al. developed a model which correlated lead surface concentration with the Pb ore grade. They predicted that an ore containing as low as 0.1% galena could resulted in 50% recovery of sphalerite flotation.

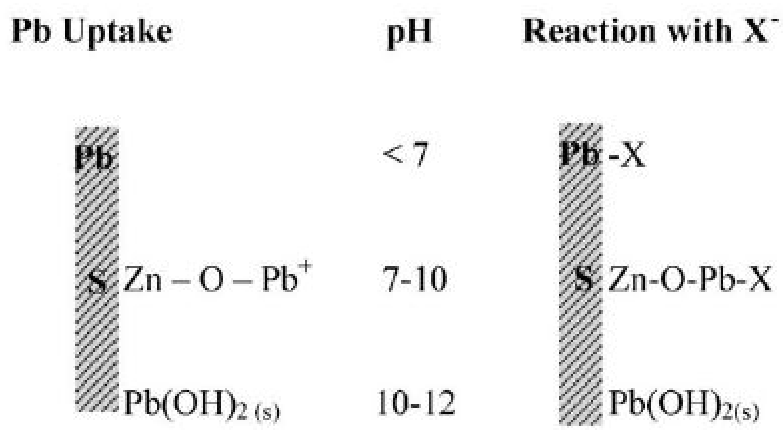

Figure 2.1 Summarized Pb activation and xanthate adsorption mechanism (Rashchi et al., 2002)

2.2.2 Formation of Zn-O-Pb surface product

Pattrick et al. (1998) suggested another possible lead activation mechanism under mildly acidic media. X-ray absorption spectroscopy (XAS) was applied in their study to determine the local structural environment of specific elements. Atomistic computer simulations demonstrated that the direct sorption of lead ions onto the sphalerite surface was energetically unfavorable. The lead ions would neither migrate into the bulk ZnS lattice nor bond to the S on the surface. Rather they suggested that the adsorption of lead ions would be facilitated by bonding to oxygen, forming Zn-O-Pb type of surface product and reaction with some of the lead oxide to form PbS species.

2.2.3 Filling empty cation sites

Popov et al. (Popov, Vučinić, Strojek, & Denca, 1989) suggested that in an acidic media, other than the exchange reaction taking place between aqueous lead ions and surface zinc ions, an additional adsorption of lead ion on the surface was found from their electrokinetic data. They proposed that the dissolution of zinc ions into solution would leave free cation sites, which provided space for aqueous lead ions to fit in.

2.3 Depression of Pb-activated sphalerite by chemicals

Many researchers have studies on the depression of metal activated sphalerite by applying different chemicals. Hereby a few of them are reviewed. It should be noticed that most of the studies were undertaken in an alkaline environment as most of the plants are operated in higher pH; however, our study will focus on the depression of Pb-activated sphalerite under mildly acidic to neutral pH (pH 6.5), as acquired by the Red Dog plant operation.

In general, the deactivation by chemicals would be categorized into two principal mechanisms: "blocking" mechanism and "cleaning" mechanism. "Blocking" mechanism suggests a formation of hydrophilic product that would prevent the adsorption of collector, whereas the "cleaning" mechanism indicates a removal of activating metal ions through the formation of precipitate/complex or soluble species. (Rashchi, Finch & Sui, 2004)

2.3.1 Zinc sulfate

El-Shall et al. (2000) studied the effect of zinc sulfate in the depression of lead-activated sphalerite. They conducted flotation tests and showed that zinc sulfate significantly depressed the lead-activated sphalerite flotation. In the absence of zinc sulfate the lead-activated sphalerite did not float beyond pH 9, while with addition of zinc sulfate the flotation could be completely depressed at pH 7.6. The flotation results interpreted that lead-activated sphalerite and galena had similar flotation behaviors, while the zeta potential measurements demonstrated that the lead-activated sphalerite surface may have intermediate properties between those of sphalerite and galena surfaces. Depression of lead-activated sphalerite in the absence of zinc sulfate was found when pH was below 3 and above 9. Those phenomena were caused by collector decomposition at very acidic pH and precipitation of lead carbonate at alkaline pH. Thermodynamic calculations were also performed by El-Shall et al., and they suggested the main depression mechanism can be displayed by the following equation, which is thermodynamically favorable from the calculation:

$$PbS_{(surface)} + Zn^{2+} \rightleftharpoons ZnS + Pb^{2+}$$

Their calculations corroborated the proposal of Fuerstenau and Metzger (1960), which stated that the lead activation could be prevented when the ratio of Zn^{2+}/Pb^{2+} was over 10^2.

2.3.2 Organic compounds

Rashchi et al. (2004) have tested the depression effect of diethylenetriamine (DETA), dextrin and carbonate on lead-contaminated sphalerite. Their performance was compared by xanthate adsorption measurement. With Pb activation, the xanthate adsorption was boosted from ca. 2×10^{-6} M/g mineral to 20×10^{-6} M/g mineral. With the three deactivators tested, the xanthate adsorption dropped to less than 10×10^{-6} M/g of sphalerite, where the order of effectiveness was found as the following: dextrin > carbonate > DETA. Zeta potential measurement was conducted to study their possible deactivation mechanism, and in each case the blocking mechanism through complex formation was proposed. Dextrin may react with zinc hydroxy and lead hydroxy species; DETA would adsorb onto the sphalerite surface and meanwhile form Pb-DETA complex. The action of carbonate was not clearly interpreted from zeta potential results, but a blocking mechanism was proposed as well.

2.3.3 Polyphosphate

Rashichi and Finch (2006) compared the performance of some chemicals as deactivators on the deactivation of lead-activated sphalerite at pH 9. They found that among DETA, sodium bicarbonate ($NaHCO_3$), silica sol, sodium phosphate ($Na_3PO_4 \cdot 12H_2O$) and sodium polyphosphate (PP), the latter one had the best deactivation effect. They applied sodium polyphosphate with an average of 17 PO_3 groups (MW=1773.3 g/mol) and the flotation recovery was reduced to less than 5% with only 1 ppm addition. From XPS and SEM studies, they concluded that polyphosphate worked by a cleaning mechanism by forming Pb-PP complexes to remove the lead ions. (Rashchi & Finch, 2002) However, polyphosphate would work less effective if it was added after the xanthate adsorption. The presence of calcium could also have impact on the performance of polyphosphate as the calcium ions would compete with lead ions to form metal-polyphosphate complexes. Rashichi and Finch also estimated a model to calculate the amount of polyphosphate required to remove Pb from the surface of ores. They found out that the economic application of polyphosphate was restricted to ores containing less than 0.1% Pb.

2.4 References

Basilio, C. I., Kartio, I. J., & Yoon, R. H. (1996). Lead activation of sphalerite during galena flotation. *Minerals Engineering*, *9*(8), 869–879. https://doi.org/10.1016/0892-6875(96)00078-7

El-Shall, H. E., Elgillani, D. A., & Abdel-Khalek, N. A. (2000). Role of zinc sulfate in depression of lead-activated sphalerite. *International Journal of Mineral Processing*, *58*(1–4), 67–75. https://doi.org/10.1016/S0301-7516(99)00055-1

Finkelstein, N. P., & Allison, S. A. (1976). *Flotation, A.M. Gaudin Memorial Volume*. (M. C. Fuerstenau, Ed.). New York, N.Y.

Fuerstenau, D. W., & Metzger, P. H. (1960). Activation of sphalerite with lead ions in the presence of zinc salts. *Transactions of the Metallurgical Society of AIME.*, *217*, 119–123.

Houot, R., & Raveneau, P. (1992). Activation of sphalerite flotation in the presence of lead ions. *International Journal of Mineral Processing*, *35*(3–4), 253–271. https://doi.org/10.1016/0301-7516(92)90037-W

Laskowski, J. S., Liu, Q., & Zhan, Y. (1997). Sphalerite activation: Flotation and electrokinetic studies. *Minerals Engineering*, *10*(8), 787–802. https://doi.org/10.1016/S0892-6875(97)00057-5

Mielczarski, J. (1986). The role of impurities of sphalerite in the adsorption of ethyl xanthate and its flotation. *International Journal of Mineral Processing*, *16*, 179–194.

Pattrick, R. A. D., Charnock, J. M., England, K. E. ., Mosselmans, J. F. W., & Wright, K. (1998). Lead sorption on the surface of ZnS with relevance to flotation: A fluorescence REFLEXAFS study. *Minerals Engineering*, *11*(11), 1025–1033.

Popov, S. R., Vučinić, D. R., & Kacanik, J. V. (1989). Floatability and adsorption of ethyl xanthate on sphalerite in an alkaline medium in the presence of dissolved lead ions. *International Journal of Mineral Processing*, *27*, 205–219.

Popov, S. R., Vučinić, D. R., Strojek, J. W., & Denca, A. (1989). Effect of dissolved lead ions on the ethylxanthate adsorption on sphalerite in weakly acidic media. *International Journal of Mineral Processing*, *27*, 51–62.

Ralston, J., Alabaster, P., & Healy, T. W. (1981). Activation of zinc sulphide with CuII, CdII and PbII: III. The Mass-spectrometric determination of elemental sulphur. *International Journal of Mineral Processing*, *7*, 279–310.

Ralston, J., & Healy, T. W. (1980a). Activation of zinc sulphide with CuII, CdIIand PbII: I. Activation in weakly acidic media. *International Journal of Mineral Processing*, *7*(3), 175–201. https://doi.org/10.1016/0301-7516(80)90016-2

Ralston, J., & Healy, T. W. (1980b). Activation of zinc sulphide with CuII, CdIIand PbII: II. Activation in neutral and weakly alkaline media. *International Journal of Mineral Processing*, *7*(3), 203–217. https://doi.org/10.1016/0301-7516(80)90017-4

Rashchi, F., & Finch, J. A. (2002). Lead-polyphosphate complexes. *Canadian Metallurgical Quarterly*, *41*(1), 1–6. https://doi.org/10.1179/cmq.2002.41.1.1

Rashchi, F., & Finch, J. A. (2006). Deactivation of Pb-contaminated sphalerite by polyphosphate. *Colloids and Surfaces A: Physicochemical and Engineering Aspects*, *276*(1–3), 87–94.

Rashchi, F., Finch, J. A., & Sui, C. (2004). Action of DETA, dextrin and carbonate on lead-contaminated sphalerite. *Colloids and Surfaces A: Physicochemical and Engineering Aspects*, *245*(1–3), 21–27. https://doi.org/10.1016/j.colsurfa.2004.05.018

Rashchi, F., Sui, C., & Finch, J. A. (2002). Sphalerite activation and surface Pb ion concentration. *International Journal of Mineral Processing*, *67*(1–4), 43–58. https://doi.org/10.1016/S0301-7516(02)00005-4

Trahar, W. J., Senior, G. D., Heyes, G. W., & Creed, M. D. (1997). The activation of sphalerite by lead -- a flotation perspective. *International Journal of Mineral Processing*, *49*, 121–148. https://doi.org/10.1016/S0301-7516(96)00041-5

Chapter 3 Materials and Experimental Techniques

3.1 Materials and reagents

High purity of sphalerite and galena minerals were purchased from Ward's Natural Science. The chemical assay of the mineral samples was determined by conducting X-ray fluorescence (XRF) analysis, and the chemical compositions of sphalerite and galena were displayed in Table 3.1 and 3.2 respectively. Sphalerite has a purity of 95.5% and galena has a purity of 99.1%. Each mineral was crushed by a jaw crusher to -2.5 mm, hand-sorted to remove impurities, and then grinded using an agate mortar/pestle grinder. The pulverized minerals were dry screened by 75 µm and 38 µm sieves. Fractions with particle size -75+38 µm were collected for micro-flotation tests, and fractions -38 µm were saved for surface analyses. The -75+38 µm minerals were ultrasonic cleaned to remove fine particles and oxidized surface layers (Clarke et al., 1995). Deionized (DI) water was added into a beaker with mineral samples. After sonication for 1 minute following by another 1 minute settling down, the supernatant was discarded. The process kept repeating until the supernatant was clear and the cleaned minerals were vacuum dried in the freeze dryer. To minimize sample oxidation, the minerals were separated into small bags, each containing ca. 1 g of the mineral, then vacuum-sealed into a large bag and stored in the freezer. Prior to each batch of the flotation test, the mineral was sonicated again in DI water for 5 minutes, and the water was discarded afterwards.

Table 3.1 Chemical assay of the sphalerite sample

Element	Zn	S	Fe	Mn	Pb	Co	Cu	Cr
Composition	62.68	32.81	3.77	0.24	0.22	0.13	0.11	0.05

Table 3.2 Chemical assay of the galena sample

Element	Pb	S	Ca	V	Cr	Fe
Composition	86.05	13.05	0.38	0.26	0.15	0.13

All reagents were of analytical grade with the highest purity accessible. The solutions were prepared with Milli-Q water (Millipore deionized, >18.2 MΩcm, 0.22 μm filtered) throughout the experiments. All solutions were prepared immediately prior to the tests and residuals were properly discarded afterwards.

3.2 Characterization techniques

3.2.1 X-ray fluorescence spectroscopy (XRF)

X-ray fluorescence spectroscopy (XRF) is a useful EDAX (Energy Dispersive X-ray Analysis) technique to quickly and non-destructively determine the chemistry of the sample provided. It allows qualitative and quantitative analysis for the chemical composition of the materials.

XRF operates by measuring the fluorescence emitted from the sample when it is irradiated by high energy X-rays. When the specimen is excited by an X-ray with sufficient energy emitted from the controlled X-ray tube, an electron will be rejected from the inner orbital shell. To stabilize the atom, an electron from higher orbital shell will move to the inner shell to fill the vacancy, at the meantime releasing extra energy as a fluorescent X-ray. The energy of this X-ray is equal to the energy difference between the two quantum shells, and is specific for each element, making the fluorescence as a unique and characteristic “fingerprint” to the element.

In this study, Orbis PC Micro-EDXRF Elemental Analyzer was used to determine the chemical compositions of sphalerite and galena samples.

3.2.2 Fourier transform infrared spectroscopy (FTIR)

Fourier transform infrared (FTIR) is a simply-operated spectroscopy that is commonly used in qualitative determination of chemical compositions of a sample. When the IR (infrared) wave is emitted from the IR source, some of the radiation can be absorbed by the sample whereas some will transmit through. The molecule will vibrate when it absorbs IR radiation with same frequency as the natural vibration frequency. Each chemical bond or functional group has its own signature frequency of absorption, so the “fingerprint” spectra can be observed for every different molecule. In this study, FTIR-ATR was applied for surface characterization. Attenuated total reflectance (ATR) is a type of sampling technique used in conjunction with FTIR spectroscopy, which allows direct sample contact with the substrate crystal in liquid or solid state without further sample preparation. Thermo Scientific™ Nicolet™ iS50 FTIR Spectrometer and a diamond reflection element with an angle of incidence of 45° were used for the experiment. The FTIR-ATR technique provides a fast and non-destructive analysis which allows determination of known and unknown chemicals, and it is easily handled as it is internally calibrated and hence does not require any calibration from the operators.

3.2.3 X-ray photoelectron spectroscopy (XPS)

X-ray photoelectron spectroscopy (XPS), also known as electron spectroscopy chemical analysis (ESCA), is a powerful technique to provide non-destructive identification of elements (except H and He) in 10 nm depth into the sample. It can not only semi-quantitively determine the chemical composition of surface element, but can also provide information about molecular environment, such as oxidation state and bonded atoms. XPS applies “soft” x-ray (100-2000eV) for analysis of core levels. (Flaim, 2017)

XPS operates based on the photoelectric effect. When an X-ray beam is shot to an atom, photon with enough energy will interact with atomic orbital electron by transferring its total energy to the electron, resulting in emission of the electron from the atom. Each electron has its unique kinetic energy, which will be collected and analyzed based on the following equation:

$$BE = hv - KE$$

Where BE represents the binding energy of electron in an atom, KE represents the kinetic energy of the emitted electron which will be measured from the detector, and hv stands for the energy from the X-ray source. The XPS spectrum will be given in the form of intensity vs. BE, where element compositions can be analyzed from the area of the spectrum at specific binding energies.

In this study, the XPS analyses were carried out with an AXIS 165 X-ray photoelectron spectrometer (Kratos Analytical) using a monochromatic Al Kα source.

3.2.4 Time-of-flight secondary ion mass spectroscopy (ToF-SIMS)

Secondary ion mass spectroscopy (SIMS) is a highly sensitive technique to analyze the chemical composition of solid surfaces and thin films to a depth of 1 to 2 nm. It can also distinguish isotopes of elements, which cannot be done by XPS. However, it may cause some extent of damage to the sample surface.

For the SIMS analysis, the solid surface is bombarded with a pulsed primary ion beam. The secondary ions, which can be either atomic or molecular, will be liberated from the surface through the bombardment and extracted. The mass to charge ratio of these ejected secondary ions will be measured by a mass spectrometer to determine the elemental, isotopic, molecular compositions. Time-of-flight mass spectroscopy (TOFMS) is a method of mass spectroscopy, which determines the mass to charge ratio based on the ions' time of flight to the detector.

In this research, ION-TOF GmbH ToF-SIMS spectrometer was used.

3.3 Micro-flotation

Micro-flotation is a very simple and straight-forward way to examine the effects of different factors on the mineral flotation, as well as to simulate real conditions in the plant.

There are two types of flotation cells that are widely applied in research studies: Hallimond tube and Denver cell. Hallimond tube is preferred to use for pure mineral flotation, which requires a small amount of minerals (a few grams) and produces relatively consistent results. Denver cell is preferred in use for plant simulation, which requests large amount of minerals (hundreds of grams). Minerals that are directly sent from the industry are often used for Denver cell flotation. In this study, Hallimond tube was used for the experiment to study pure mineral flotation behavior.

A custom built Hallimond tube was used for micro-flotation tests, as shown in Figure 3.1. The Hallimond tube is composed of two parts, of which the upper part A is the main body used for flotation and concentrate collection, and the bottom part B is used as a gas inlet. A glass frit with pore size of 1.6 μm is embedded in part B so that nitrogen gas could pass through. A magnetic stirrer bar is placed right above the glass frit to enable the agitation of the slurry. As marked in the figure, position 2 is connected to a high purity nitrogen cylinder and a flowmeter was used to control the gas flow rate. The narrow throat connecting the concentrate vessel and the vertical tube allows only one bubble to pass through at a time, which minimizes the entrainment.

Conditioning of the minerals was completed outside the Hallimond tube. Every single batch of flotation required 1 g of minerals, unless otherwise stated. The minerals were placed in a beaker and agitated with 150 mL Milli-Q water, and pH of the solution was adjusted to pH 6.5. After each reagent addition, the minerals were conditioned for 5 min and then followed by the next reagent addition. The pH was maintained at 6.50 ± 0.05 by addition of A.C.S. grade hydrochloric acid (HCl) and sodium hydroxide (NaOH). The pulp was immediately transferred into the cell through the feed inlet (position 1 in Fig. 3.1) after conditioning was finished. The stirring speed of the magnetic bar was set at 700 rpm. Nitrogen gas flow rate was controlled by Cole-Parmer® gas mass flowmeter at 30 sccm (standard cubic centimeters). Each batch of flotation lasted for 5 minutes. At the end of the flotation, concentrate was collected from position 3 in Figure 3.1, and tailing remaining in the cell was rinsed with Milli-Q water and collected. Concentrate and tailing were filtered, dried in the oven overnight and weighed separately.

For single mineral flotation, the recovery can be calculated as the following:

$$Recovery\% = \frac{Mass\ of\ concentrate}{Mass\ of\ concentrate + Mass\ of\ tailing} \times 100\%$$

For mixed minerals flotation, the concentrate and tailing had to be analyzed by XRF after weighing to determine the chemical compositions. Take Zn recovery as an example, it can be calculated by the equation:

$$Zn\ \% = \frac{Mass\ of\ concentrate \times Zn\%\ (c)}{Mass\ of\ concentrate \times Zn\%\ (c) + Mass\ of\ tailing \times Zn\%\ (t)} \times 100\%$$

Where Zn% (c) denotes the zinc composition in the concentrate, and Zn% (t) represents the zinc assay in tailing. The lead recovery could be analyzed and calculated in a similar manner.

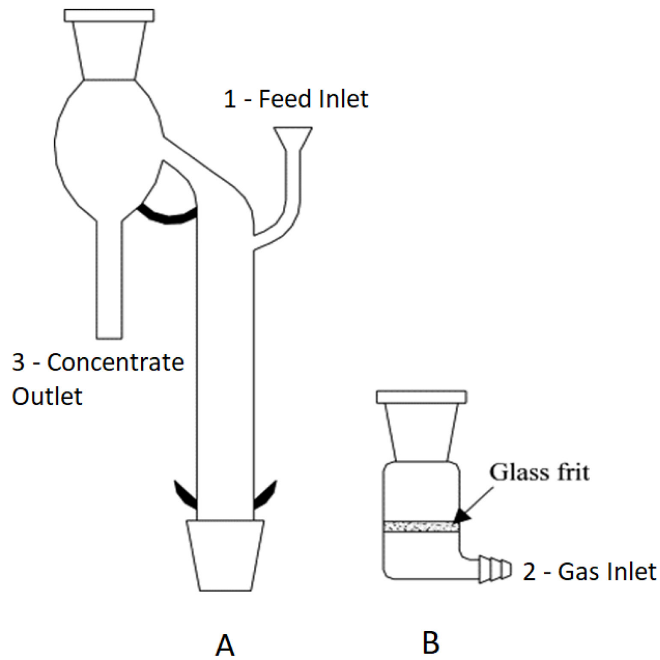

Figure 3.1 Schematic of Hallimond tube (Chachula & Liu, 2003)

3.4 References

Chachula, F., & Liu, Q. (2003). Upgrading a rutile concentrate produced from Athabasca oil sands tailings. *Fuel*, *82*(8), 929–942. https://doi.org/10.1016/S0016-2361(02)00401-5

Clarke, P., Fornasiero, D., Ralston, J., & Smart, R. S. C. (1995). A study of the removal of oxidation products from sulfide mineral surfaces. *Minerals Engineering*, *8*(11), 1347–1357. https://doi.org/10.1016/0892-6875(95)00101-U

Flaim, E. (2017). *Surface spectroscopy -- Introduction to XPS, AES, SIMS, and EDS*.

Chapter 4 Micro-flotation Under Neutral pH

4.1 Single mineral flotation

4.1.1 Sphalerite

The 95.5% sphalerite was floated with and without lead ions and potassium ethyl xanthate (KEX) at pH 6.5 to observe its flotation behavior, and the results are listed in Table 4.1. In the absence of collector, sphalerite had a floatability under 20% with or without Pb activation. The addition of lead ions alone did not appreciably elevate the flotation recovery. When in the absence of lead ions, the recovery was increased by 10% with KEX addition. This result was consistent with others' studies, which could be attribute to the activation by the lattice impurities. (Mielczarski, 1986; Rashchi et al., 2002; Trahar et al., 1997) When the sphalerite was treated with lead ions for 5 min prior to the addition of xanthate, the flotation recovery of sphalerite enormously increased from 18.4% to 96.4%. This huge discrepancy suggests the lead activation of sphalerite allows the adsorption of potassium ethyl xanthate, hence rendering the surface hydrophobic and floatable.

Table 4.1 Sphalerite flotation recovery with different chemicals at pH 6.5

Condition	Recovery
Collectorless	18.4%
5 min in 10^{-5} M $Pb(NO_3)_2$	19.4%
5 min in 10^{-5} M KEX	29.1%
5 min in 10^{-5} M $Pb(NO_3)_2$ + 5 min in 10^{-5} M KEX	96.4%

4.1.2 Galena

Figure 4.1 shows the galena flotation recovery with respect to the concentration of potassium ethyl xanthate. Under collectorless flotation, galena had a recovery of 14.6%, suggesting that galena is originally hydrophilic. With addition of only 5 x 10^{-6} M (50 ppm) KEX, the recovery boosted to 92.8%, which indicates that xanthate can easily adsorb onto the galena surface without any activation. The recovery remained constant at about 93% within 1% of experiment error upon increased xanthate addition amount.

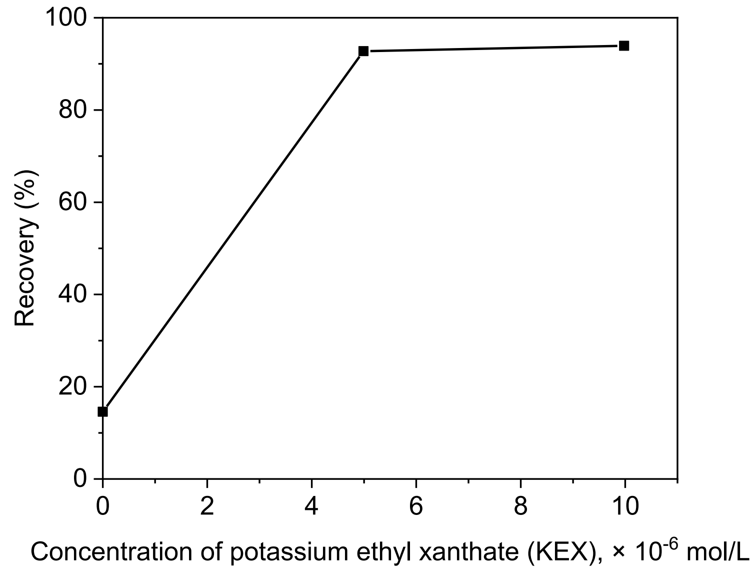

Figure 4.1 Flotation recovery of galena with change of potassium ethyl xanthate concentration

4.2 Single mineral flotation with sodium hydrogen phosphate

To examine the depression effect of sodium hydrogen phosphate (Na_2HPO_4), flotation tests of Pb-activated sphalerite and galena were conducted respectively, as shown in Figure 4.2 and 4.3.

In Fig. 4.2, flotation recovery of Pb-activated sphalerite was shown with the increase of sodium hydrogen phosphate concentration. Prior to the flotation test, the sphalerite was conditioned in the following sequence: 10^{-5} M lead nitrate ($Pb(NO_3)_2$), Na_2HPO_4 with varied concentration, and finally 10^{-5} M KEX. After each chemical addition, the sphalerite was conditioned for 5 min. The results showed that with addition of 10^{-5} M Na_2HPO_4, the flotation recovery dropped significantly from 97.8% to 50.5%, which was a considerable depression. The flotation recovery progressively decreased as the concentration of Na_2HPO_4 was increased, reaching 46.8% when the phosphate concentration was 10^{-3} M.

The red dot that was plotted in Fig. 4.2 demonstrated the copper activation of Pb-activated sphalerite that was treated with sodium hydrogen phosphate. The conditioning sequence was: 10^{-5} M $Pb(NO_3)_2$, 10^{-3} M Na_2HPO_4, 10^{-5} M copper sulfate ($CuSO_4$), and lastly 10^{-5} M KEX. It can be seen that even with a high amount of phosphate addition (10^{-3} M), the sphalerite still could be re-activated by copper ions, hitting a recovery of 97.0%. This result suggests that the addition of sodium hydrogen phosphate has effective deactivation of sphalerite due to Pb ions but not Cu ions, which is a satisfactory finding, as the addition of sodium hydrogen phosphate would not affect the sphalerite flotation (re-activated by Cu) in the zinc rougher afterwards.

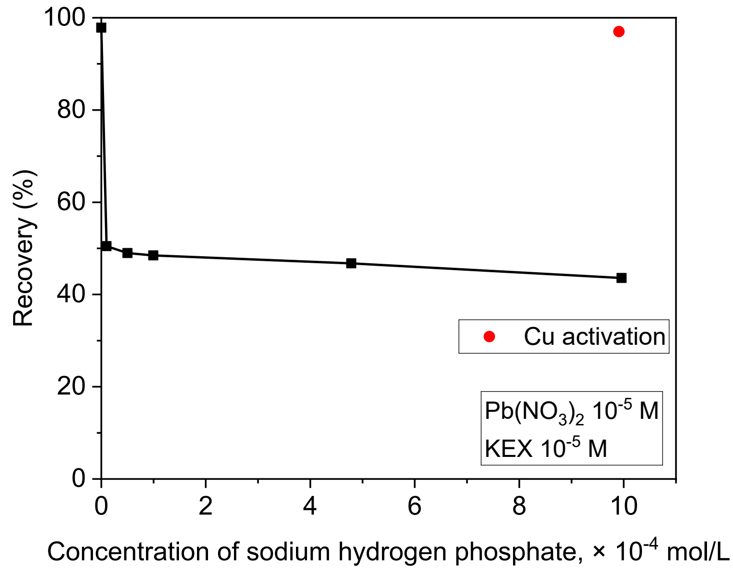

Figure 4.2 Flotation recovery of Pb-activated sphalerite with change of sodium hydrogen phosphate concentration

Figure 4.3 demonstrates the flotation behavior of galena by varying sodium hydrogen phosphate concentration. Galena was condition in Na_2HPO_4 first followed by KEX, each for 5 minutes. The graph showed that the addition of sodium hydrogen phosphate would not have any depression effect on galena flotation. The recovery remained above 93% as the Na_2HPO_4 concentration was increased, up to 5 x 10^{-4} M.

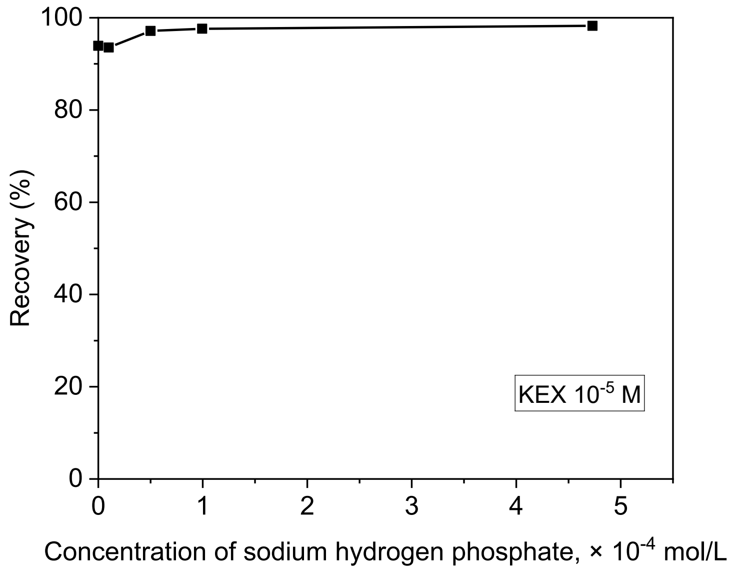

Figure 4.3 Flotation recovery of galena with change of sodium hydrogen phosphate concentration

From the above flotation results, it is concluded that sodium hydrogen phosphate has considerable effect on depression of Pb-activated sphalerite but does not impact the galena flotation at all. Hence it is expected that sodium hydrogen phosphate may have a good performance in the selective flotation of mixed sphalerite-galena minerals.

4.3 Mixed mineral flotation with sodium hydrogen phosphate

For mixed mineral flotation tests, 1 g of sphalerite and 1 g of galena were mixed together. Figure 4.4 shows the flotation results with addition of 10^{-5} M KEX. At no phosphate addition, both sphalerite and galena completely floated at a recovery of 98.6%. This high recovery of sphalerite indicates the inadvertent activation of sphalerite by Pb ions from dissolution of galena. (Basilio, Kartio & Yoon, 1996) With sodium hydrogen phosphate addition, there was no significant depression on galena flotation. The Pb% recovery remained at around 97% as the concentration of sodium hydrogen phosphate was increased. Sphalerite flotation recovery slowly dropped down as the phosphate concentration grew up. However, unlike the single mineral flotation, Zn% recovery still hit at 85.6% when 4.79 x 10^{-4} M of Na_2HPO_4 was added. The mixed flotation result did not show a good selectivity as expected and would not be satisfactory for sphalerite depression in a lead rougher. The reason causing this phenomenon will be evaluated based on the surface analyses presented in the next chapter.

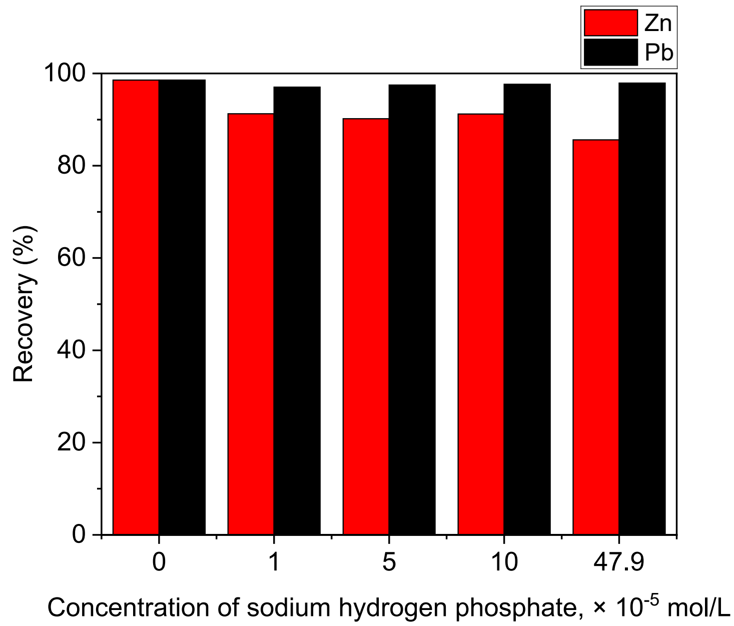

Figure 4.4 Mixed mineral flotation recovery with change of sodium hydrogen phosphate concentration, [KEX]=10^{-5} M

4.4 Sphalerite flotation with zinc sulfate

To study the reason for the mixed mineral flotation not reaching expectation, the ability of sodium hydrogen phosphate reacting with lead ion was studied. Figure 4.5 demonstrates the flotation recovery change of Pb-activated sphalerite with a fixed amount (10^{-5} M) of Na_2HPO_4 when the lead concentration was increased. When the Pb^{2+} concentration was from 10^{-5} M to 5 x 10^{-5} M, the sphalerite recovery remained at ca. 50%. As the lead concentration rose to 9.88 x 10^{-5} M, the recovery increased sharply to 89.0%.

Beyond a Pb^{2+} concentration of 4.75×10^{-4} M, sphalerite floated completely at 98.1% and sodium hydrogen phosphate had no depression effect at all. This result indicates that sodium hydrogen phosphate has limited ability to react with lead ions and may not be sufficient to cause an effective depression during the mixed mineral flotation. Therefore, further treatment of sphalerite is required.

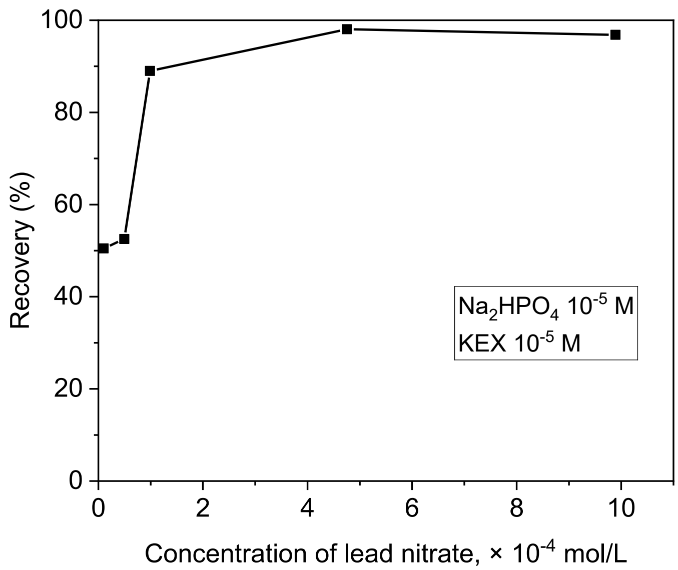

Figure 4.5 Flotation recovery of Pb-activated sphalerite with change of lead nitrate concentration

To compensate the lacked ability of sodium hydrogen phosphate reacting with lead ions, zinc sulfate was chosen to treat the sphalerite prior to addition of phosphate in this study. Zinc sulfate has been widely applied as a depressant in Pb-Zn separation. Although zinc sulfate was not found efficient in depression of sphalerite flotation caused by Cu or Ag activation, it worked effectively in controlling the Pb activation. (El-Shall et al., 2000; Fuerstenau & Metzger, 1960; Ranchev, Grigorova & Nishkov, 2016) We would expect zinc sulfate to react on the Pb-activated surface first, so that the amount of adsorbed Pb ions is decreased and sodium hydrogen phosphate would achieve an ideal depression effect.

Figure 4.6 demonstrates the flotation behavior of Pb-activated sphalerite as the Zn^{2+} concentration changes. The conditioning sequence for sphalerite was: 10^{-5} M $Pb(NO_3)_2$, zinc sulfate ($ZnSO_4$) with varying concentration, and lastly 10^{-5} M KEX. Initially without addition of Zn ions, Pb-activated sphalerite floated at 97.8%. As zinc sulfate was introduced from 10^{-5} M to 10^{-3} M, the sphalerite recovery dropped slowly from 97.2% to 89.5%. When the concentration of zinc sulfate was increased to 5 x 10^{-5} M, a lower recovery of 73.5% was achieved. The flotation recovery gradually decreased and levelled at 70.5% when 0.05 M of zinc sulfate was added. Unlike others' studies (El-Shall et al., 2000; Ranchev et al., 2016) which showed a significant depression of Pb-activated sphalerite upon adding zinc sulfate, the result presented in Fig. 4.6 suggested that zinc sulfate had a limited depression effect. The reason causing the discrepancy could be resulted from many aspects, such as different minerals selected for flotation, the way of grinding, different methods for mineral conditioning, different pH selected for experiments, and so on.

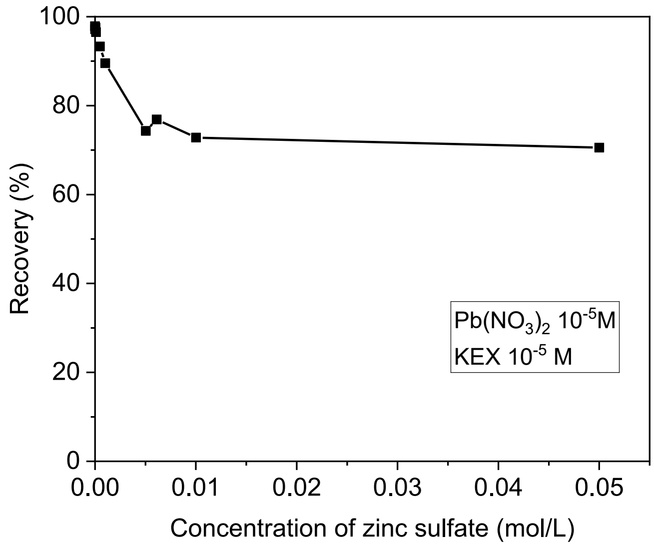

Figure 4.6 Flotation recovery of Pb-activated sphalerite with change of zinc sulfate concentration

Figure 4.7 shows the depression effect on Pb-activated sphalerite with combination usage of sodium hydrogen phosphate and zinc sulfate. The zinc concentration was fixed at 0.005 M and the concentration of Na_2HPO_4 was changed. The conditioning sequence was as the following: 10^{-5} M $Pb(NO_3)_2$, 0.005 M $ZnSO_4$, Na_2HPO_4 with varying concentration, and lastly 10^{-5} M KEX. Sphalerite was conditioned for 5 min after each chemical addition. It can be observed from the graph that with 0.005 M $ZnSO_4$ and 10^{-5} M Na_2HPO_4, the flotation recovery dropped significantly to 21.3%. The recovery continued to decrease slowly as Na_2HPO_4 concentration was increased, reaching 17.3% when

Na_2HPO_4 concentration rose to 9.46 x 10^{-4} M. This graph suggests that the combination usage of sodium hydrogen phosphate and zinc sulfate has a much more impressive depression on sphalerite flotation than using any of these reagents alone, and hence it is worth trying to apply this combination into the mixed mineral flotation for testing.

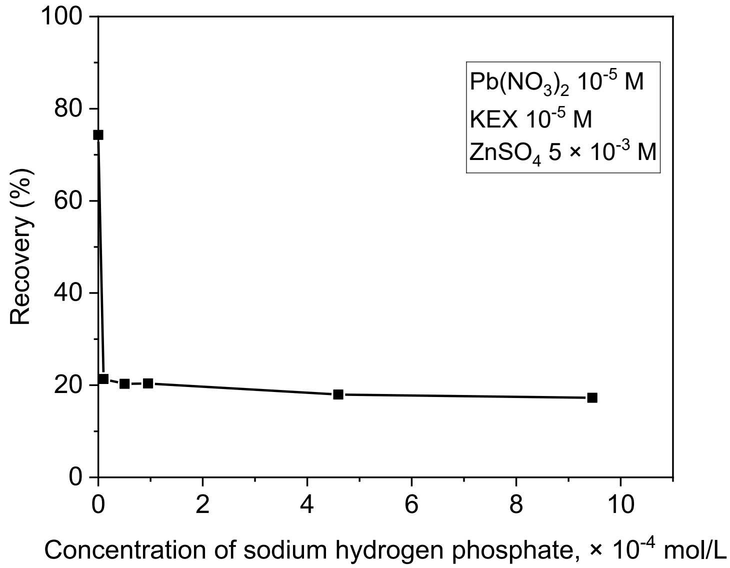

Figure 4.7 Flotation recovery of Pb-activated sphalerite with change of sodium hydrogen phosphate concentration, pre-treated with 0.005M $ZnSO_4$

4.5 Selective flotation with combined usage of sodium hydrogen phosphate and zinc sulfate

Based on the good depression result performed on the Pb-activated sphalerite flotation by using sodium hydrogen phosphate and zinc sulfate, it is reasonable to test whether this combination would be feasible in depression when applied in a mixed mineral system.

Figure 4.8 shows the mixed flotation recoveries by fixing the zinc sulfate concentration at 0.005 M (same condition as the sphalerite flotation) and varying the concentration of sodium hydrogen phosphate. When there was no Na_2HPO_4 addition and the mixed mineral system was treated with 0.005 M $ZnSO_4$ alone, the recovery of Zn and Pb was 90.0% and 97.6%, respectively. The recoveries remained constant with Na_2HPO_4 addition of up to 3×10^{-6} M, and Zn% recovery dropped to 78.3% at $[Na_2HPO_4] = 4 \times 10^{-6}$ M. When the phosphate concentration was raised to 6×10^{-6} M, a significant depression of sphalerite was recognized, resulting in a Zn% recovery of 27.2%. However, starting from this point, a depression on galena was also observed. The Pb% recovery decreased from ca. 98% at lower Na_2HPO_4 concentration to 78.8%. The sodium hydrogen phosphate had stronger depression effect on both sphalerite and galena flotation as the concentration was increased. When $[Na_2HPO_4] = 5 \times 10^{-4}$ M, a full depression on both minerals was observed, resulting in 10.2% recovery of Zn and 22.2% recovery of Pb. Here the mixed flotation results showed that using zinc sulfate alone would not have a good effect on selective flotation, while with the combination usage of Na_2HPO_4 and 0.005 M $ZnSO_4$ together, the depression effect would be to strong so that even galena would be depressed. A balanced amount of the two reagents should be sought for the best selectivity.

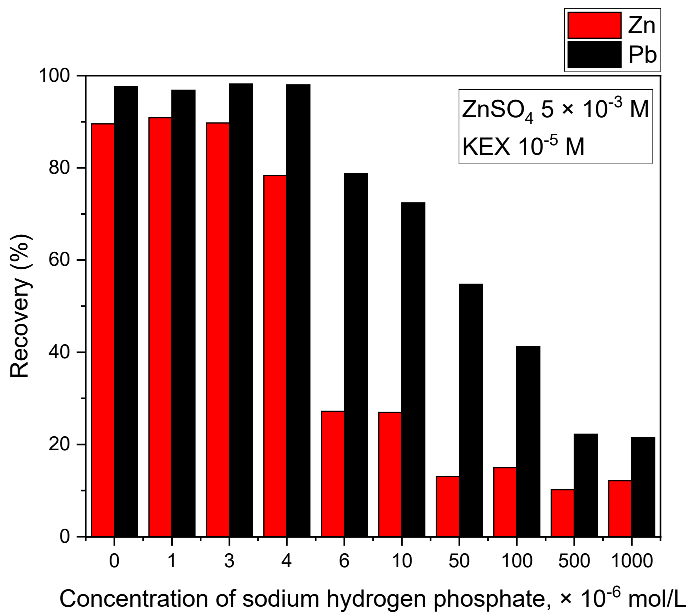

Figure 4.8 Mixed mineral flotation recovery with change of sodium hydrogen phosphate concentration, pre-treated with 0.005M $ZnSO_4$

A fixed amount of Na_2HPO_4 at 10^{-5} M was used and zinc sulfate concentration was altered in order to achieve the best selectivity. The mixed flotation results were displayed in Fig. 4.9. It is observed that with decreased amount of zinc sulfate, the Pb-Zn selectivity was greatly enhanced. The optimum selectivity was achieved when the concentration of both sodium hydrogen phosphate and zinc sulfate was 10^{-5} M, in this case the Zn% recovery dropped to 55.0% and the Pb% recovery remained at 90.2%.

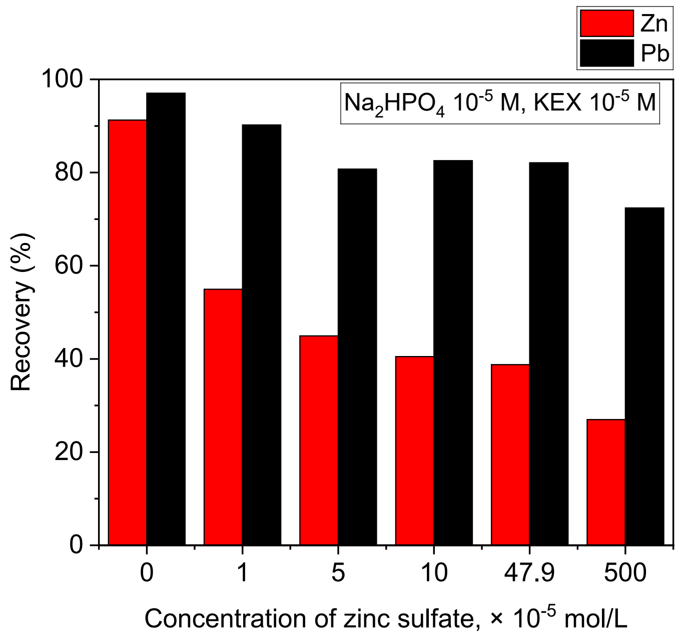

Figure 4.9 Mixed mineral flotation recovery with change of zinc sulfate concentration, [Na_2HPO_4] = 10^{-5} M

4.6 References

Basilio, C. I., Kartio, I. J., & Yoon, R. H. (1996). Lead activation of sphalerite during galena flotation. *Minerals Engineering*, *9*(8), 869–879. https://doi.org/10.1016/0892-

6875(96)00078-7

El-Shall, H. E., Elgillani, D. A., & Abdel-Khalek, N. A. (2000). Role of zinc sulfate in depression of lead-activated sphalerite. *International Journal of Mineral Processing*, *58*(1–4), 67–75. https://doi.org/10.1016/S0301-7516(99)00055-1

Fuerstenau, D. W., & Metzger, P. H. (1960). Activation of sphalerite with lead ions in the presence of zinc salts. *Transactions of the Metallurgical Society of AIME.*, *217*, 119–123.

Mielczarski, J. (1986). The role of impurities of sphalerite in the adsorption of ethyl xanthate and its flotation. *International Journal of Mineral Processing*, *16*, 179–194.

Ranchev, M., Grigorova, I., & Nishkov, I. (2016). Zinc depression in the galena flotation of Erma Reka concentrator. In *24th World Mining Congress Proceedings* (pp. 339–348).

Rashchi, F., Sui, C., & Finch, J. A. (2002). Sphalerite activation and surface Pb ion concentration. *International Journal of Mineral Processing*, *67*(1–4), 43–58. https://doi.org/10.1016/S0301-7516(02)00005-4

Trahar, W. J., Senior, G. D., Heyes, G. W., & Creed, M. D. (1997). The activation of sphalerite by lead -- a flotation perspective. *International Journal of Mineral Processing*, *49*, 121–148. https://doi.org/10.1016/S0301-7516(96)00041-5

Chapter 5 Depression Mechanisms of Lead-activated Sphalerite by Sodium Hydrogen Phosphate and Zinc Sulfate

5.1 Introduction

From the flotation results presented in Chapter 4, sodium hydrogen phosphate has been shown a satisfactory effect on depression of lead activated sphalerite flotation. The mixed mineral flotation also showed Pb-Zn selectivity with the combination usage of sodium hydrogen phosphate and zinc sulfate at their equilibrium amount. It is essential to study why the two reagents would work as depressants to the flotation system.

The deactivation mechanism was studied by conducting surface characterizations, utilizing Fourier Transform Infrared (FTIR) spectroscopy, X-ray Photoelectron Spectroscopy (XPS), and Time-of-Flight Secondary Ion Mass Spectroscopy (ToF-SIMS).

5.2 Experiment method and sample preparation

5.2.1 FTIR measurement

The infrared spectra were recorded by Thermo Scientific™ Nicolet™ iS50 FTIR Spectrometer. A diamond reflectance element was used. The spectra were collected for a wavenumber range from 400 to 4000 cm^{-1}.

The 95.5% sphalerite was crushed to above 10 mm × 5 mm in size. The specimen was polished by hand using silicon carbide grinding discs until the surface was completely flat with no defects. The sphalerite sample was first sonicated for 5 min to avoid surface oxidation prior to each test. Typically, for each reagent addition, the sphalerite was immersed in the solution for 20 min. Afterwards the solution would be decanted, and the sphalerite sample was thoroughly washed with Milli-Q (MQ) water. This step ensures that the peaks observed from the IR spectra are truly due to the adsorption of certain compounds onto the surface, rather than the residual solution remained on the surface. The pH value was maintained at 6.50 ± 0.05 over the entire conditioning process by adding hydrochloric acid and sodium hydroxide.

5.2.2 XPS measurement

The XPS analyses were performed on a Kratos AXIS 165 X-ray photoelectron spectrometer, using a monochromatic Al Kα X-ray (1486.6 eV) as incident beam.

For the sample preparation, 2 g of sphalerite with particle size <38 μm was used. The mineral was sonicated in DI water for 5 min right before each sample preparation. The mineral sample was conditioned in each reagent solution (150 mL) for 10 min. After each conditioning, sphalerite was filtered and washed thoroughly with MQ water. The filtered powder would be then transferred to the beaker for the next conditioning. When the conditioning process was finished, the powdered will be freeze dried under vacuum. Dried samples were mounted on non-conductive tape for XPS analyses.

The XPS spectra were analyzed with Casa XPS software. The binding energy of C 1s at 284.8 eV was used for calibration.

5.2.3 ToF-SIMS measurement

ToF-SIMS measurements were conducted by ION-TOF GmbH ToF-SIMS spectrometer. The sample preparation followed the procedure as describe in section 5.2.2.

5.3 Results and discussion

5.3.1 FTIR measurement

Figure 5.1 compares the IR spectra of Pb-activated sphalerite in the presence of 10^{-3} M KEX with and without the treatment of sodium hydrogen phosphate. The conditioning sequence for the sphalerite sample was as the following: $Pb(NO_3)_2$, Na_2HPO_4, and KEX. Each solution had a concentration of 10^{-3} M.

The adsorption of lead ethyl xanthate can be examined by the positions and shapes of the high frequency -C-O-C- xanthate band, which appears at a wavenumber at ca. 1200

cm^{-1}. The lead ethyl xanthate peak is normally observed as an overlap of two bands: 1195 cm^{-1} and 1207 cm^{-1}, which represent the monolayer and multilayer forms of lead ethyl xanthate, respectively. (Leppinen & Mielczarski, 1986; Mielczarski, 1986; Poling, 1976; Popov & Vučinić, 1988; Popov et al., 1989) From Fig. 5.1(a) a characteristic peak at 1195.45 cm^{-1} was observed, which represented the monolayer form of lead ethyl xanthate. The characteristic peak for multilayer form at 1207 cm^{-1} was not observed from the spectrum. Greenler (1962) and Poling and Leja (1963) claimed that the first (or a few) monolayer(s) of lead ethyl xanthate was formed by the 1:1 coordination between the lead ion and the xanthate ion, i.e. in the form of Pb-EtX. The 1:2 coordination product, $Pb(EtX)_2$ appears in the multilayer form. Therefore, it can be concluded that the monolayer form of lead ethyl xanthate (Pb-EtX) was the dominant species on the sphalerite surface at pH 6.5. A characteristic band of ethyl dixanthogen at about 1265 cm^{-1} (J. O. Leppinen, 1990; Poling & Leja, 1963) was not observed from the spectrum.

Figure 5.1(b) shows no obvious peaks over the wavenumber range 900-1400 cm^{-1}, which indicates that the addition of sodium hydrogen phosphate prevents the adsorption of lead ethyl xanthate onto the sphalerite surface.

By comparing the two spectra in Fig. 5.1, it is concluded that lead ion that adsorbs on the sphalerite surface can easily bond with ethyl xanthate to form lead ethyl xanthate in monolayer form under near neutral pH (pH 6.5). The product formed is hydrophobic and hence will increase the sphalerite flotation recovery. When the Pb-activated sphalerite was treated with sodium hydrogen phosphate, there was no lead ethyl xanthate observed on the surface. Whether the prohibited formation was caused by blocking or cleaning mechanism will be furtherly discovered.

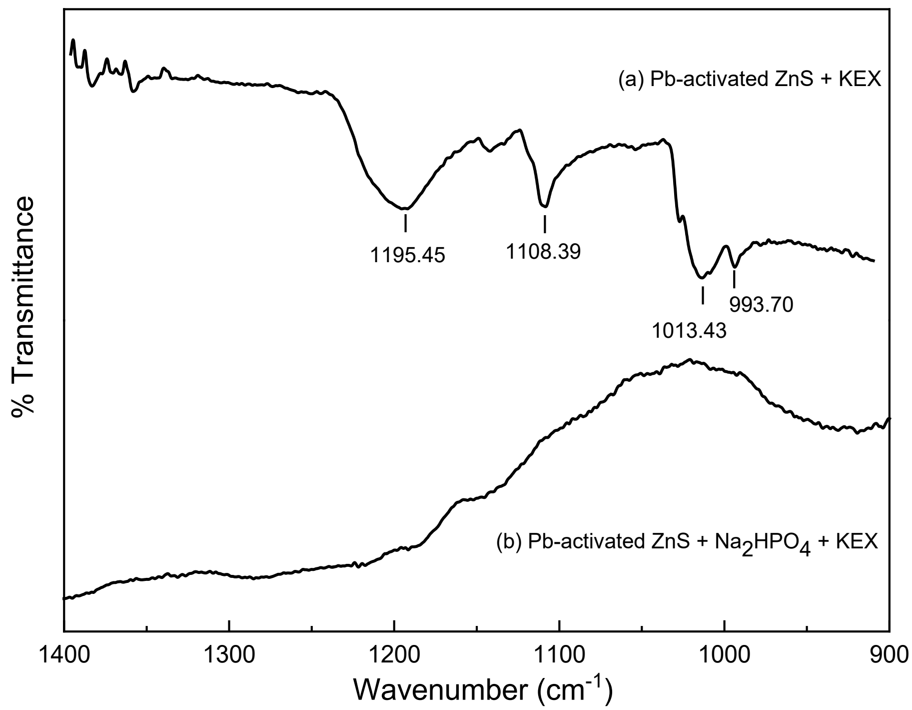

Figure 5.1 IR spectra of Pb-activated sphalerite in the presence of (a) 10^{-3} M KEX; (b) 10^{-3} M Na_2HPO_4 and 10^{-3} M KEX

5.3.2 XPS measurement

Detailed narrow scan of Pb 4f peaks were displayed in Figures 5.2-5.5. The peaks located at ca. 137.5 eV and 142.0 eV in all of the four figures are characteristic bands for Pb $4f_{7/2}$ and Pb $4f_{5/2}$ in the form of PbS. (Houot & Raveneau, 1992; Mielczarski, 1986) Some slight discrepancies in binding energies could be due to the variations in conductivities of the samples (Kartio, Basilio, & Yoon, 1998), which may vary from level of impurities in the sample. (Chen, Chen, & Guo, 2010) It should be noted that there existed superposition of Pb 4f and Zn 3s (located at ca. 139.6 eV) bands at the scanned region for Pb 4f, so the atomic area of Zn 3s should be subtracted when taking account in calculating the atomic concentration. (Basilio et al., 1996; Houot & Raveneau, 1992; Mielczarski, 1986)

Figure 5.2 shows the Pb 4f scan spectrum for an unactivated sphalerite sample. The Pb 4f peaks were noticed due to the lead impurities inherently borne in the sphalerite lattice.

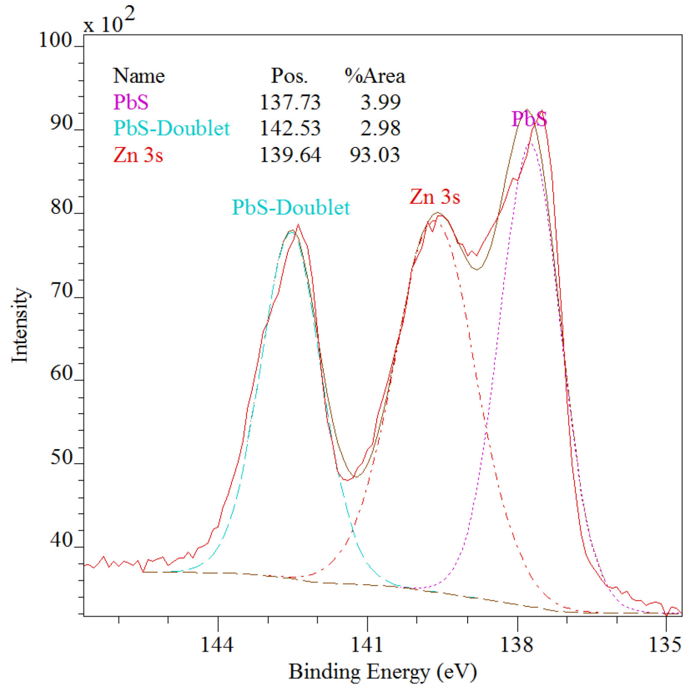

Figure 5.2 Pb(4f) XPS spectrum of unactivated sphalerite

The spectra were similar in both shapes and values for sphalerite sample with or without KEX addition, when lead concentration of 10^{-5} M was introduced, as shown in Fig. 5.3. In comparison with Fig. 5.2, an additional doublet was found at 138.2 eV and 143.0 eV. The 0.6 eV higher energy shift relative to PbS was correlated to the formation of lead oxide (PbO). (Alan N. Buckley & Woods, 1984; Houot & Raveneau, 1992) This new doublet appeared suggests that upon lead activation, part of the PbS was oxidized to PbO. The oxidized portion was relatively low, as can be calculated based on the %area from the spectra, 67.65% of Pb detected was in the form of PbS, while 32.35% of Pb appeared in the form of PbO.

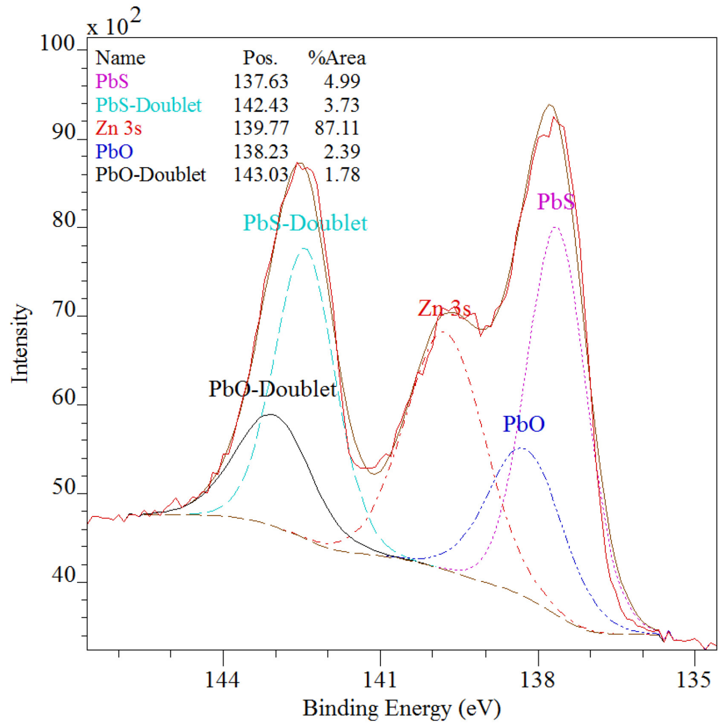

Figure 5.3 Pb(4f) XPS spectrum of Pb-activated sphalerite, [KEX] = 10^{-5} M

When sodium hydrogen phosphate was introduced to the system, as shown in Fig. 5.4, a lower intensity of Pb was observed, suggesting a partial removal of Pb ions by sodium hydrogen phosphate. Meanwhile a significant increase of PbO was also observed. Calculating from the %area, only 30.99% of the total Pb amount remained as in the form of PbS, whereas 69.01% was converted into the PbO form.

From the above results it can be concluded that sodium hydrogen phosphate can prevent Pb adsorption onto the sphalerite surface to some extent, and meanwhile cause oxidation of Pb ions to render the sphalerite surface hydrophilic.

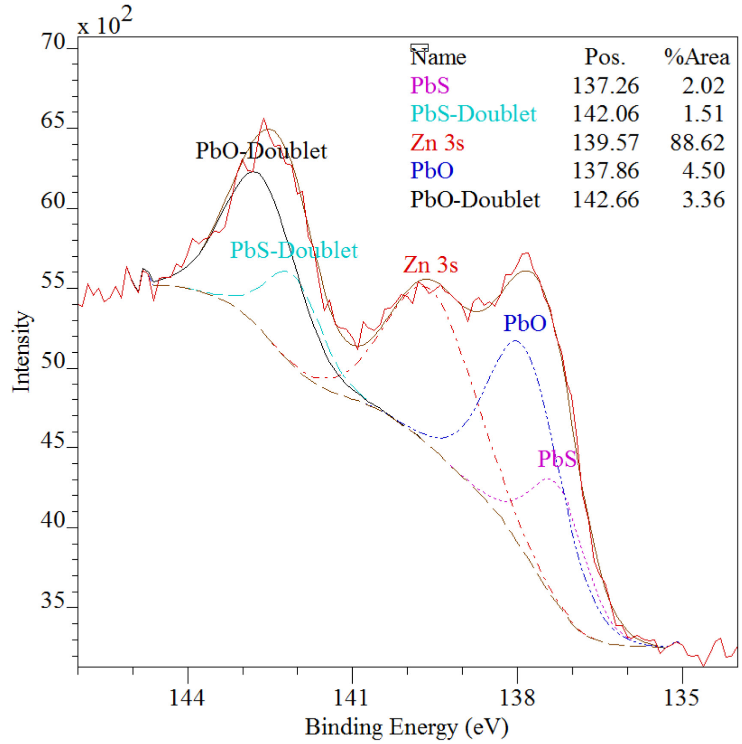

Figure 5.4 Pb(4f) XPS spectrum of Pb-activated sphalerite with treatment of sodium hydrogen phosphate, [KEX] = 10^{-5} M

Figure 5.5 displays the Pb 4f XPS spectrum for the Pb-activated sphalerite that was treated with 0.005 M $ZnSO_4$, 5 x 10^{-5} M Na_2HPO_4, and 10^{-5} M KEX. A furtherly decreased Pb intensity was noticed comparing to the signal as shown in Fig. 5.4, suggesting less Pb adsorption on the sphalerite surface. Here 48.27% of Pb was in the form of PbS and 51.73% of Pb was in the form of PbO. The decreased PbO/PbS ratio compared to Fig. 5.4 may be due to the treatment with zinc sulfate prior to addition of sodium hydrogen phosphate. The addition of zinc sulfate somehow inhibited the adsorption of Pb ions onto the sphalerite surface, possibly due to le Chatelier's principle. Le Chaterlier's principle states that when a system at equilibrium is subjected to a disturbance, such as change in concentration, temperature, or pressure, the system will adjust itself to partially counteract the change. In this case, the exchange reaction between Zn and Pb ions are expressed as the following equation:

$$Pb^{2+} + ZnS_{(surface)} \rightleftharpoons PbS + Zn^{2+}$$

When a significant amount of Zn ions was added to the system, the equilibrium of this reversible reaction would be shifted to the left-hand side, hence it would be harder for Pb ions to exchange with Zn ions on the surface.

The addition of zinc sulfate reduced the Pb adsorption on the sphalerite surface, and consequently decreased the amount of PbO. (Notice that there was about 32.33% Pb oxidation occurred immediately after Pb activation.) This might explain why the PbO/PbS ratio was lower (1.156) when zinc sulfate and sodium hydrogen phosphate were applied together, comparing to the ratio (2.227) when sodium hydrogen phosphate worked alone. Table 5.1 listed the PbO/PbS ratios for all conditions for a clearer overview.

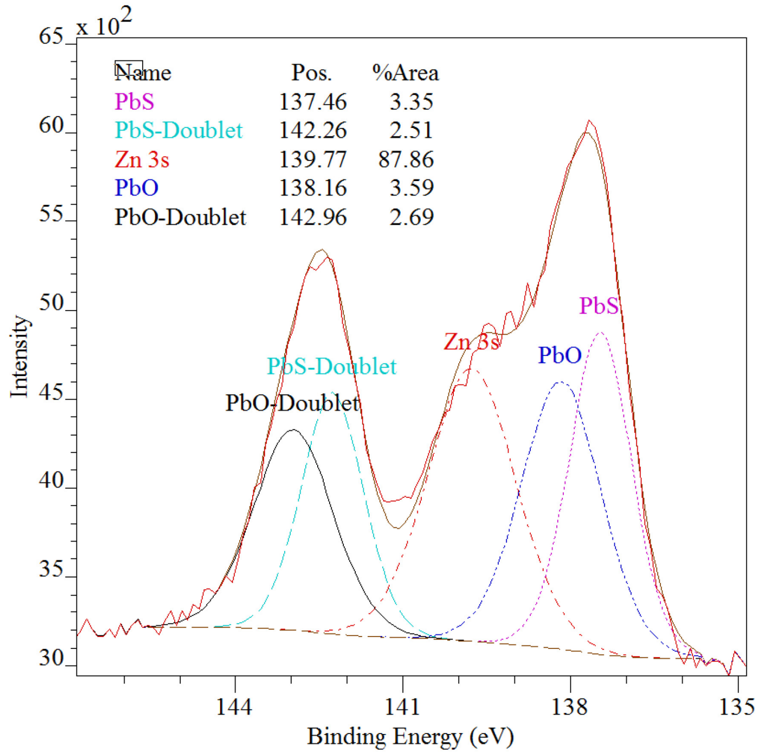

Figure 5.5 Pb(4f) XPS spectrum of Pb-activated sphalerite with treatment of sodium hydrogen phosphate and zinc sulfate, [KEX] = 10^{-5} M

Table 5.1 Percentage atomic concentration of Pb in the form of sulfide and oxide analyzed by XPS and their ratios under different conditions

%Atomic Concentration	Pb in PbO	Pb in PbS	PbO/PbS
Pure Sphalerite	0	100	0
Pb-activated sphalerite	33.21	66.79	0.497
Pb-activated Sp + KEX	32.35	67.65	0.478
Pb-activated Sp + Na_2HPO_4 + KEX	69.01	30.99	2.227
Pb-activated Sp + $ZnSO_4$ + Na_2HPO_4 + KEX	53.61	46.39	1.156

The XPS spectra for element S 2p of Pb-activated sphalerite under different conditions were plotted in Fig. 5.6-5.9. For sphalerite with or without lead activation, only one set of S 2p doublet was observed at a binding energy of 161.5 eV for $2p_{3/2}$ peak, as shown in Fig.5.6. This doublet stands for sulfur in the form of sulfide, i.e. S^{2-}. (Buckley et al., 1989; Buckley & Woods, 1984; Kartio et al., 1998; Laajalehto et al., 1991; Mielczarski, 1986) The lead activation would not change the concentration or bonding structure of S atoms.

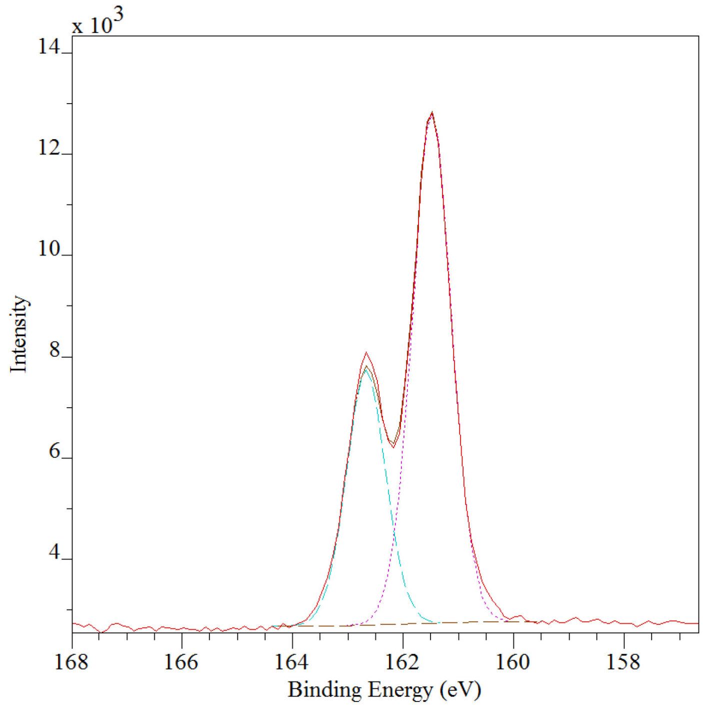

Figure 5.6 S(2p) XPS spectrum of Pb-activated sphalerite

When sodium ethyl xanthate was added to the Pb-activated sphalerite, another S 2p doublet located at 162.4 eV with low intensity was observed, as shown in Fig. 5.7. This doublet could be caused by two products: lead ethyl xanthate (Laajalehto et al., 1991; Laajalehto et al., 1993; Mielczarski, 1986), or oxidation product of the activated sphalerite (Kartio et al., 1998). Both of the products are highly possibly formed. The IR spectrum has shown obvious characteristic peaks for the formation of lead ethyl xanthate; meanwhile the XPS spectra for Pb 4f element showed oxidation occurred once the sphalerite surface was activated by Pb ion.

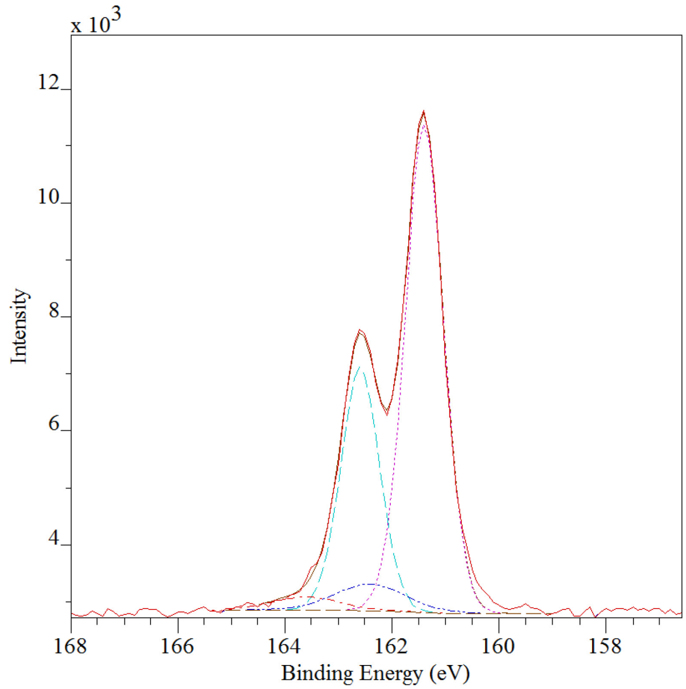

Figure 5.7 S(2p) XPS spectrum of Pb-activated sphalerite, [KEX] = 10^{-5} M

In Figure 5.8, other than the two doublets found at 161.5 eV and 162.4 eV, which stand for S^{2-} and $Pb(EtX)_2$/oxidation product of Pb-activated sphalerite, respectively, there was one more set of S 2p doublet found from the scan, which was very broad over the range of 163-170 eV, centering at about 166 eV, as shown in Fig. 5.8. Since the peaks are too broad, it is hard to determine which exact form of sulfur the peaks correspond to. From the literature, some oxidized forms of S: elemental sulfur or sulfur in polysulfides S^0, thiosulfate $S_2O_3^-$, and sulfate SO_4^{2-}, were found at binding energies 164.3 eV, 163.9 eV and 167.9 eV respectively. (Buckley & Woods, 1984; Houot & Raveneau, 1992; Laajalehto et al., 1993) Although we cannot determine what exactly was formed, it is certain that oxidation of sulfur was occurring on the surface upon sodium hydrogen phosphate addition.

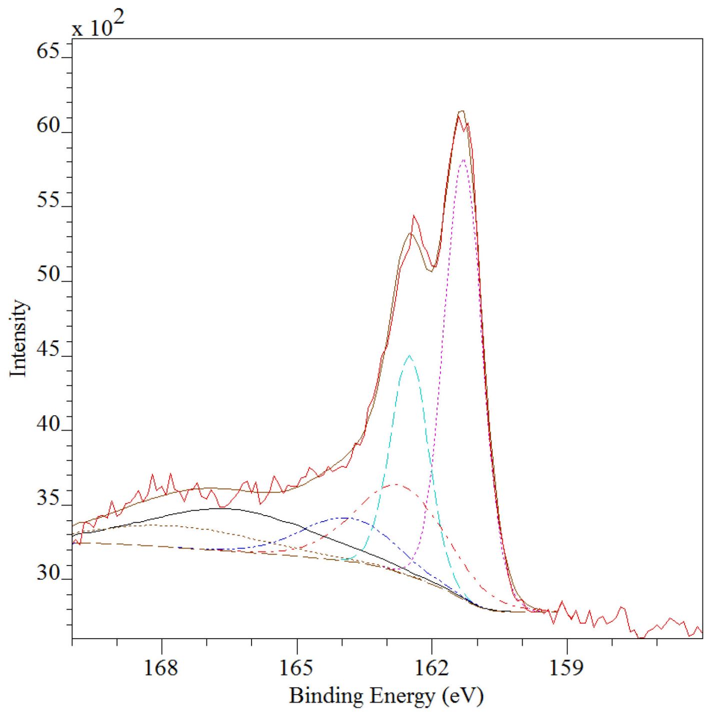

Figure 5.8 S(2p) XPS spectrum of Pb-activated sphalerite with treatment of sodium hydrogen phosphate, [KEX] = 10^{-5} M

5.3.3 ToF-SIMS measurement

Table 5.2 presents the ToF-SIMS analysis result on Pb signals in the form of PbS and PbO. The table shows very similar trend for PbO/PbS ratios at different conditions in comparison with Table 5.1. In both of the tables, the PbO/PbS ratio was nearly zero for an unactivated pure sphalerite. ToF-SIMS has higher sensitivity than XPS, so a very low amount of PbO was detected. As sphalerite was activated by Pb ions, partial oxidation of PbS into PbO was observed. The addition of xanthate to the lead activated sphalerite would not cause considerable oxidation of PbS, according to the similar PbO/PbS ratios (1.842 vs. 1.959) before and after KEX addition. The addition of sodium hydrogen phosphate strongly stimulated the increase of lead oxide, suggesting that sodium hydrogen phosphate possesses oxidizing ability over lead ions. A decreased PbO/PbS ratio when the sodium hydrogen phosphate and zinc sulfate were in combined use suggested that zinc sulfate first reduced the amount of Pb ions adsorbing onto the sphalerite surface, and hence decreasing the direct oxidation of PbS.

Table 5.2 Signal intensity PbS and PbO and their ratios analyzed by ToF-SIMS under different conditions

Signal Intensity	PbO^-	PbS^-	PbO/PbS
Pure Sphalerite	9	46	0.196
Pb-activated sphalerite	140	76	1.842
Pb-activated Sp + KEX	145	74	1.959
Pb-activated Sp + Na_2HPO_4 + KEX	331	74	4.473
Pb-activated Sp + $ZnSO_4$ + Na_2HPO_4 + KEX	145	55	2.636

5.3 Conclusion

Based on the surface characterizations conducted above, the depression mechanisms of Pb-activated sphalerite by using sodium hydrogen phosphate and zinc sulfate can be concluded.

Sodium hydrogen phosphate acted partially by a cleaning mechanism but blocking mechanism would be dominant. The addition of sodium hydrogen phosphate would partially remove Pb ions by forming complexes, however, this amount is minor and would not mainly contribute to the depression. The main mechanism was by oxidizing PbS into PbO, and therefore forming a hydrophilic oxide layer on the sphalerite surface. Oxidation of sulfur was also observed with the addition of sodium hydrogen phosphate.

Zinc sulfate worked as depressant according to le Chatelier's principle. For the Pb-Zn exchange reaction, as the zinc concentration was increased, the equilibrium would be shifted to an opposite side, hence increasing difficulty for Pb ions to adsorb onto the sphalerite surface.

5.4 References

Buckley, A. N., & Woods, R. (1984). An X-ray photoelectron spectroscopic study of the oxidation of galena. *Applications of Surface Science*, *17*, 401–414.

Buckley, A. N., Woods, R., & Wouterlood, H. J. (1989). An XPS investigation of the surface of natural sphalerites under flotation-related conditions. *International Journal of Mineral Processing*, *26*(1–2), 29–49. https://doi.org/10.1016/0301-7516(89)90041-0

Chen, Y., Chen, J., & Guo, J. (2010). A DFT study on the effect of lattice impurities on the electronic structures and floatability of sphalerite. *Minerals Engineering*, *23*(14), 1120–1130. https://doi.org/10.1016/j.mineng.2010.07.005

Greenler, R. G. (1962). An infrared investigation of xanthate adsorption by lead sulfide. *Journal of Physical Chemistry*, *66*(5), 879–883. https://doi.org/10.1021/j100811a028

Houot, R., & Raveneau, P. (1992). Activation of sphalerite flotation in the presence of lead ions. *International Journal of Mineral Processing*, *35*(3–4), 253–271. https://doi.org/10.1016/0301-7516(92)90037-W

Kartio, I. J., Basilio, C. I., & Yoon, R. H. (1998). An XPS study of sphalerite activation by copper. *Langmuir*, *14*(18), 5274–5278. https://doi.org/10.1021/la970440c

Laajalehto, K., Nowak, P., Pomianowski, A., & Suoninen, E. (1991). Xanthate adsorption at PbS/aqueous interfaces: Comparison of XPS, infrared and electrochemical results. *Colloids and Surfaces*, *57*(2), 319–333. https://doi.org/10.1016/0166-6622(91)80165-K

Laajalehto, K., Nowak, P., & Suoninen, E. (1993). On the XPS and IR identification of the products of xanthate sorption at the surface of galena. *International Journal of Mineral Processing*, *37*(1–2), 123–147. https://doi.org/10.1016/0301-7516(93)90009-Y

Leppinen, J., & Mielczarski, J. (1986). Spectroscopic study of the adsorption of thiol collectors on lead sulphide in the presence of sodium sulphide. *International Journal of Mineral Processing*, *18*(1–2), 3–20. https://doi.org/10.1016/0301-7516(86)90003-7

Leppinen, J. O. (1990). FTIR and flotation investigation of the adsorption of ethyl xanthate on activated and non-activated sulfide minerals. *International Journal of Mineral Processing*, *30*(3–4), 245–263. https://doi.org/10.1016/0301-7516(90)90018-T

Mielczarski, J. (1986). The role of impurities of sphalerite in the adsorption of ethyl xanthate and its flotation. *International Journal of Mineral Processing*, *16*, 179–194.

Poling, G. W. (1976). Reactions between thiol reagents and sulphide minerals. In *M.C. Fuerstenau (Editor), Flotation, A.M. Gaudin Memorial Volume* (p. 350). New York, N.Y.: AIME.

Poling, G. W., & Leja, J. (1963). Infrared study of xanthate adsorption on vacuum deposited films of lead sulfide and metallic copper under conditions of controlled oxidation. *Journal of Physical Chemistry*, *67*(10), 2121–2126. https://doi.org/10.1021/j100804a036

Popov, S. R., & Vučinić, D. R. (1988). Influence of lead ions on the adsorption characteristics of galena in flotation. *Colloids and Surfaces*, *30*(2), 387–400.

https://doi.org/10.1016/0166-6622(88)80139-2

Popov, S. R., Vučinić, D. R., Strojek, J. W., & Denca, A. (1989). Effect of dissolved lead ions on the ethylxanthate adsorption on sphalerite in weakly acidic media. *International Journal of Mineral Processing*, *27*, 51–62.

Chapter 6 Conclusion and Future Work

6.1 Major conclusion

In this study, the activation of sphalerite by lead ions under a near neutral pH (pH 6.5) was studied. Sodium hydrogen phosphate with the combination usage of zinc sulfate was considered for sphalerite depression. Micro-flotation tests using Hallimond tube were conducted to examine the flotation behavior of sphalerite, galena and their mixed mineral under different conditions. Surface characterizations, such as FTIR, XPS, and ToF-SIMS were performed to understand the activation and deactivation mechanisms.

The major findings from this research are listed as the following:

1. At pH 6.5, sphalerite floated poorly without metal activation, no matter in the presence or absence of xanthate. With Pb activation, sphalerite flotation responded well upon addition of potassium ethyl xanthate.
2. Sodium hydrogen phosphate was found effective in depressing Pb-activated sphalerite and caused no effect on galena flotation. However, there was no significant depression on either sphalerite or galena in the mixed mineral flotation with addition of sodium hydrogen phosphate.
3. With the combined addition of sodium hydrogen phosphate and zinc sulfate, a better depression was observed for Pb-activated sphalerite than using sodium

hydrogen phosphate alone. The combined usage also showed effective depression during the mixed mineral flotation. The best selectivity was achieved when both sodium hydrogen phosphate and zinc sulfate were at a concentration of 10^{-5} M, in this case the Zn% recovery dropped to 55.0% while the Pb% recovery remained at 90.2%.

4. The FTIR spectra showed that with lead activation and potassium ethyl xanthate addition, characteristic peaks of lead ethyl xanthate were observed. The result suggests that Pb ions adsorbed on sphalerite surface and bonded with the xanthate ions to form hydrophobic lead ethyl xanthate. When sodium hydrogen phosphate was added to the system, the signature peaks of lead ethyl xanthate were not observed from the IR spectrum, which indicates the addition of sodium hydrogen phosphate prevented the formation of lead ethyl xanthate.

5. Similar conclusions were drawn from XPS and ToF-SIMS analyses. When Pb ions were added to sphalerite, a small portion of PbS was oxidized to PbO. When sodium hydrogen phosphate was added to the system, a massive oxidation of PbS to PbO was observed. When zinc sulfate was added to the system prior to sodium hydrogen phosphate, the amount of PbO decreased. Sodium hydrogen phosphate worked as a depressant mainly by oxidizing PbS into hydrophilic PbO, and it had limited ability to react with Pb ion to prevent its adsorption onto the sphalerite

surface. Zinc sulfate worked according to le Chatelier's principle. When a high concentration of zinc sulfate was added, it will create difficulty for Pb ion to exchange with Zn ion on the surface layer of sphalerite.

6.2 Suggestions for future work

This study has shed a light on using sodium hydrogen phosphate for depression of Pb-activated sphalerite. However, there are still some questions that are not answered and many other aspects to be explored. Some suggestions are listed below:

1. Although the mechanism of sodium hydrogen phosphate was confirmed as an oxidation process, it is not clear how exactly the reaction is undergoing. It is worth trying to apply more surface characterizations to investigate into the reaction process.
2. There have been some researches using various phosphate compounds to complex with Ca ions in the processing solution or in the mineral lattice and some of them were found effective. It is necessary to consider whether there will be a competition between Ca and Pb ions to react with sodium hydrogen phosphate. Simulated process water is suggested to use in order to study the effect of phosphate in a more complex environment.

Bibliography

Basilio, C. I., Kartio, I. J., & Yoon, R. H. (1996). Lead activation of sphalerite during galena flotation. *Minerals Engineering*, *9*(8), 869–879. https://doi.org/10.1016/0892-6875(96)00078-7

Buckley, A. N., & Woods, R. (1984). An X-ray photoelectron spectroscopic study of the oxidation of galena. *Applications of Surface Science*, *17*, 401–414.

Buckley, A. N., Woods, R., & Wouterlood, H. J. (1989). An XPS investigation of the surface of natural sphalerites under flotation-related conditions. *International Journal of Mineral Processing*, *26*(1–2), 29–49. https://doi.org/10.1016/0301-7516(89)90041-0

Chachula, F., & Liu, Q. (2003). Upgrading a rutile concentrate produced from Athabasca oil sands tailings☆. *Fuel*, *82*(8), 929–942. https://doi.org/10.1016/S0016-2361(02)00401-5

Chen, Y., Chen, J., & Guo, J. (2010). A DFT study on the effect of lattice impurities on the electronic structures and floatability of sphalerite. *Minerals Engineering*, *23*(14), 1120–1130. https://doi.org/10.1016/j.mineng.2010.07.005

Clarke, P., Fornasiero, D., Ralston, J., & Smart, R. S. C. (1995). A study of the removal of oxidation products from sulfide mineral surfaces. *Minerals Engineering*, *8*(11), 1347–1357. https://doi.org/10.1016/0892-6875(95)00101-U

Dean, J. A. (1999). *Lange's Handbook of chemistry* (5th ed.). McGraw-Hill, Inc.

Deng, M. (2013). *Impact of gypsum supersaturated solution on the flotation of sphalerite*. University of Alberta.

El-Shall, H. E., Elgillani, D. A., & Abdel-Khalek, N. A. (2000). Role of zinc sulfate in depression of lead-activated sphalerite. *International Journal of Mineral Processing*, *58*(1–4), 67–75. https://doi.org/10.1016/S0301-7516(99)00055-1

Finkelstein, N. P., & Allison, S. A. (1976). *Flotation, A.M. Gaudin Memorial Volume*. (M. C. Fuerstenau, Ed.). New York, N.Y.

Flaim, E. (2017). *Surface spectroscopy -- Introduction to XPS, AES, SIMS, and EDS*.

Fuerstenau, D. W., & Metzger, P. H. (1960). Activation of sphalerite with lead ions in the presence of zinc salts. *Transactions of the Metallurgical Society of AIME.*, *217*, 119–123.

Greenler, R. G. (1962). An infrared investigation of xanthate adsorption by lead sulfide. *Journal of Physical Chemistry*, *66*(5), 879–883. https://doi.org/10.1021/j100811a028

Houot, R., & Raveneau, P. (1992). Activation of sphalerite flotation in the presence of lead ions. *International Journal of Mineral Processing*, *35*(3–4), 253–271.

https://doi.org/10.1016/0301-7516(92)90037-W

Kartio, I. J., Basilio, C. I., & Yoon, R. H. (1998). An XPS study of sphalerite activation by copper. *Langmuir*, *14*(18), 5274–5278. https://doi.org/10.1021/la970440c

Laajalehto, K., Nowak, P., Pomianowski, A., & Suoninen, E. (1991). Xanthate adsorption at PbS/aqueous interfaces: Comparison of XPS, infrared and electrochemical results. *Colloids and Surfaces*, *57*(2), 319–333. https://doi.org/10.1016/0166-6622(91)80165-K

Laajalehto, K., Nowak, P., & Suoninen, E. (1993). On the XPS and IR identification of the products of xanthate sorption at the surface of galena. *International Journal of Mineral Processing*, *37*(1–2), 123–147. https://doi.org/10.1016/0301-7516(93)90009-Y

Laskowski, J. S., Liu, Q., & Zhan, Y. (1997). Sphalerite activation: Flotation and electrokinetic studies. *Minerals Engineering*, *10*(8), 787–802. https://doi.org/10.1016/S0892-6875(97)00057-5

Leja, J. (1982). *Surface Chemistry of Froth Rotation* (1st ed.). New York: Plenum Press.

Leppinen, J., & Mielczarski, J. (1986). Spectroscopic study of the adsorption of thiol collectors on lead sulphide in the presence of sodium sulphide. *International Journal of Mineral Processing*, *18*(1–2), 3–20. https://doi.org/10.1016/0301-

7516(86)90003-7

Leppinen, J. O. (1990). FTIR and flotation investigation of the adsorption of ethyl xanthate on activated and non-activated sulfide minerals. *International Journal of Mineral Processing*, *30*(3–4), 245–263. https://doi.org/10.1016/0301-7516(90)90018-T

Letient, H. (2017). Red Dog Operations. Retrieved from http://www.reddogalaska.com/

Mielczarski, J. (1986). The role of impurities of sphalerite in the adsorption of ethyl xanthate and its flotation. *International Journal of Mineral Processing*, *16*, 179–194.

Pattrick, R. A. D., Charnock, J. M., England, K. E. ., Mosselmans, J. F. W., & Wright, K. (1998). Lead sorption on the surface of ZnS with relevance to flotation: A fluorescence REFLEXAFS study. *Minerals Engineering*, *11*(11), 1025–1033. Retrieved from http://www.sciencedirect.com/science/article/pii/S0892687598000909

Poling, G. W. (1976). Reactions between thiol reagents and sulphide minerals. In *M.C. Fuerstenau (Editor), Flotation, A.M. Gaudin Memorial Volume* (p. 350). New York, N.Y.: AIME.

Poling, G. W., & Leja, J. (1963). Infrared study of xanthate adsorption on vacuum deposited films of lead sulfide and metallic copper under conditions of controlled oxidation. *Journal of Physical Chemistry*, *67*(10), 2121–2126.

https://doi.org/10.1021/j100804a036

Popov, S. R., & Vučinić, D. R. (1988). Influence of lead ions on the adsorption characteristics of galena in flotation. *Colloids and Surfaces*, *30*(2), 387–400. https://doi.org/10.1016/0166-6622(88)80139-2

Popov, S. R., Vučinić, D. R., & Kacanik, J. V. (1989). Floatability and adsorption of ethyl xanthate on sphalerite in an alkaline medium in the presence of dissolved lead ions. *International Journal of Mineral Processing*, *27*, 205–219.

Popov, S. R., Vučinić, D. R., Strojek, J. W., & Denca, A. (1989). Effect of dissolved lead ions on the ethylxanthate adsorption on sphalerite in weakly acidic media. *International Journal of Mineral Processing*, *27*, 51–62.

Ralston, J., Alabaster, P., & Healy, T. W. (1981). Activation of zinc sulphide with CuII, CdII and PbII: III. The Mass-spectrometric determination of elemental sulphur. *International Journal of Mineral Processing*, *7*, 279–310.

Ralston, J., & Healy, T. W. (1980a). Activation of zinc sulphide with CuII, CdIIand PbII: I. Activation in weakly acidic media. *International Journal of Mineral Processing*, *7*(3), 175–201. https://doi.org/10.1016/0301-7516(80)90016-2

Ralston, J., & Healy, T. W. (1980b). Activation of zinc sulphide with CuII, CdIIand PbII: II. Activation in neutral and weakly alkaline media. *International Journal of Mineral*

Processing, *7*(3), 203–217. https://doi.org/10.1016/0301-7516(80)90017-4

Ranchev, M., Grigorova, I., & Nishkov, I. (2016). Zinc depression in the galena flotation of Erma Reka concentrator. In *24th World Mining Congress Proceedings* (pp. 339–348).

Rao, S. R., & Leja, J. (2004). *Surface Chemistry Surface Chemistry of Froth Flotation* (2nd ed.). New York: Springer Science+Business Media.

Rashchi, F., & Finch, J. A. (2002). Lead-polyphosphate complexes. *Canadian Metallurgical Quarterly*, *41*(1), 1–6. https://doi.org/10.1179/cmq.2002.41.1.1

Rashchi, F., & Finch, J. A. (2006). Deactivation of Pb-contaminated sphalerite by polyphosphate. *Colloids and Surfaces A: Physicochemical and Engineering Aspects*, *276*(1–3), 87–94.

Rashchi, F., Finch, J. A., & Sui, C. (2004). Action of DETA, dextrin and carbonate on lead-contaminated sphalerite. *Colloids and Surfaces A: Physicochemical and Engineering Aspects*, *245*(1–3), 21–27. https://doi.org/10.1016/j.colsurfa.2004.05.018

Rashchi, F., Sui, C., & Finch, J. A. (2002). Sphalerite activation and surface Pb ion concentration. *International Journal of Mineral Processing*, *67*(1–4), 43–58. https://doi.org/10.1016/S0301-7516(02)00005-4

Trahar, W. J., Senior, G. D., Heyes, G. W., & Creed, M. D. (1997). The activation of sphalerite by lead -- a flotation perspective. *International Journal of Mineral Processing*, *49*, 121–148. https://doi.org/10.1016/S0301-7516(96)00041-5

Appendix

Selected original data from micro-flotation tests are listed in the following tables.

Table A1. Flotation recovery of sphalerite with different chemical reagents

Test No.	pH	[Pb(NO3)2] (mol/L)	[KEX] (mol/L)	[Na2HPO4] (mol/L)	[CuSO4·5H2O] (mol/L)	Recovery
1	6.45	N/A	N/A	N/A	N/A	18.20%
2	6.48	1.03E-05	N/A	N/A	N/A	19.40%
3	6.45	N/A	1.02E-05	N/A	N/A	29.10%
4	6.5	1.01E-05	9.33E-06	9.91E-04	9.2E-06	96.99%

Table A2. Flotation recovery of sphalerite with respect to concentration of sodium hydrogen phosphate, $[Pb^{2+}]$ = [KEX] = 10^{-5} M

Test No.	pH	[Pb(NO3)2] (mol/L)	[KEX] (mol/L)	[Na2HPO4] (mol/L)	Recovery
1	6.5	1.04E-05	1.03E-05	0	97.84%
2	6.53	1.01E-05	9.92E-06	1.00E-05	50.48%
3	6.53	1.01E-05	9.92E-06	5.02E-05	48.98%
4	6.54	9.95E-06	9.82E-06	9.95E-05	48.48%
5	6.49	9.58E-06	9.45E-06	4.79E-04	46.76%
6	6.55	9.06E-06	8.94E-06	9.96E-04	43.58%

Table A3. Flotation recovery of sphalerite with respect to concentration of zinc sulfate, $[Pb^{2+}]$ = [KEX] = 10^{-5} M

Test No.	pH	[Pb(NO3)2] (mol/L)	[KEX] (mol/L)	[ZnSO4·7H2O] (mol/L)	Recovery
1	6.53	1.02E-05	1.01E-05	1.03E-05	97.17%
2	6.45	1.02E-05	1.01E-05	5.15E-05	97.54%
3	6.5	1.01E-05	1.00E-05	1.02E-04	96.53%
4	6.49	9.75E-06	9.63E-06	4.91E-04	93.29%
5	6.48	9.22E-06	9.19E-06	1.02E-03	89.54%
6	6.52	1.00E-05	1.02E-05	5.02E-03	73.49%
7	6.51	1.02E-05	1.01E-05	5.04E-03	75.11%
8	6.48	1.00E-05	1.02E-05	6.12E-03	76.89%
9	6.49	1.00E-05	1.02E-05	1.00E-02	72.80%
10	6.49	1.00E-05	1.02E-05	5.00E-02	70.53%

Table A4. Flotation recovery of sphalerite with respect to concentration of sodium hydrogen phosphate, $[Pb^{2+}]$ = [KEX] = 10^{-5} M, $[Zn^{2+}]$ = 0.005 M

Test No.	pH	$[Pb(NO_3)_2]$ (mol/L)	[KEX] (mol/L)	$[ZnSO_4 \cdot 7H_2O]$ (mol/L)	$[Na_2HPO_4]$ (mol/L)	Recovery
1	6.55	1.01E-05	1.02E-05	5.06E-03	1.00E-05	21.34%
2	6.55	1.01E-05	1.01E-05	5.06E-03	5.04E-05	20.29%
3	6.53	1.01E-05	1.01E-05	5.06E-03	9.53E-05	20.36%
4	6.53	1.01E-05	1.06E-05	5.06E-03	4.59E-04	17.98%
5	6.55	1.01E-05	1.04E-05	5.06E-03	9.46E-04	17.26%

Table A5. Flotation recovery of sphalerite with respect to concentration of lead nitrate, $[Na_2HPO_4]$ = [KEX] = 10^{-5} M

Test No.	pH	$[Pb(NO_3)_2]$ (mol/L)	[KEX] (mol/L)	$[Na_2HPO_4]$ (mol/L)	Recovery
1	6.45	1E-05	1.04E-05	9.93E-06	50.48%
2	6.45	4.97E-05	1.03E-05	9.86E-06	52.51%
3	6.45	9.88E-05	1.02E-05	9.81E-06	88.99%
4	6.51	0.000475	9.84E-06	9.44E-06	98.05%
5	6.45	0.000989	1.03E-05	9.88E-06	96.83%

Table A6. Flotation recovery of galena with respect to concentration of potassium ethyl xanthate

Test No.	pH	[KEX] (mol/L)	Recovery
1	6.5	0	14.56%
2	6.48	4.99E-06	92.78%
3	6.52	4.99E-06	92.72%
4	6.46	9.98E-06	93.93%

Table A7. Flotation recovery of galena with respect to concentration of sodium hydrogen phosphate, [KEX] = 10^{-5} M

Test No.	pH	[KEX] (mol/L)	$[Na_2HPO_4]$ (mol/L)	Recovery
1	6.49	1.02E-05	1.00E-05	91.23%
2	6.45	1.02E-05	1.00E-05	93.55%
3	6.49	1.02E-05	5.02E-05	97.13%
4	6.45	1.01E-05	9.94E-05	97.63%
5	6.45	9.65E-06	4.73E-04	98.24%

Table A8. Mixed flotation recovery with respect to concentration of sodium hydrogen phosphate, [KEX] = 10^{-5} M

Test No.	pH	[KEX] (mol/L)	[Na_2HPO_4] (mol/L)	Zn Recovery	Pb Recovery
1	6.47	9.92E-06	0	98.56%	98.56%
2	6.55	9.92E-06	1.00E-05	91.25%	97.02%
3	6.49	9.92E-06	5.02E-05	90.18%	97.47%
4	6.45	9.82E-06	9.95E-05	91.21%	97.64%
5	6.47	9.45E-06	4.79E-04	85.61%	97.92%
6	6.51	8.94E-06	9.96E-04	93.18%	97.60%

Table A9. Mixed flotation recovery with various concentration of sodium hydrogen phosphate and zinc sulfate, [KEX] = 10^{-5} M

Test No.	pH	[KEX] (mol/L)	[$ZnSO_4 \cdot 7H_2O$] (mol/L)	[Na_2HPO_4] (mol/L)	Zn Recovery	Pb Recovery
1	6.53	1.00E-05	5.07E-03	0	89.53%	97.61%
2	6.47	1.01E-05	5.06E-03	1.97E-06	90.87%	96.85%
3	6.53	1.01E-05	5.06E-03	2.96E-06	89.72%	98.18%
4	6.55	1.01E-05	5.06E-03	3.94E-06	78.32%	97.98%
5	6.55	1.02E-05	5.06E-03	5.63E-06	27.20%	78.80%
6	6.53	1.02E-05	5.07E-03	1.01E-05	26.98%	72.41%
7	6.55	1.01E-05	5.07E-03	5.00E-05	13.03%	54.75%
8	6.53	1.02E-04	5.07E-03	9.47E-05	14.95%	41.24%
9	6.47	1.02E-05	5.07E-03	4.56E-04	10.17%	22.23%
10	6.55	1.02E-05	5.07E-03	9.52E-04	12.14%	21.47%